Supporting Information

A Well-Balanced Force Field *ff03CMAP* for Folded and Disordered Proteins

Yangpeng Zhang[1,#], Hao Liu[1,#], Sheng Yang[1,#], Ray Luo[2,*], and Hai-Feng Chen[1,3,*]

[1]*State Key Laboratory of Microbial metabolism, Department of Bioinformatics and Biostatistics, National Experimental Teaching Center for Life Sciences and Biotechnology, School of Life Sciences and Biotechnology, Shanghai Jiao Tong University, Shanghai, 200240, China*
[2]*Departments of Molecular Biology and Biochemistry, Chemical and Molecular Engineering, and Materials Science and Engineering, and Biomedical Engineering, University of California, Irvine, USA*
[3]*Shanghai Center for Bioinformation Technology, Shanghai, 200235, China*

[#]These authors contributed equally to this work.

*Corresponding authors
Email addresses: haifengchen@sjtu.edu.cn; ray.luo@rayluolab.org
Tel: 86-21-34204348
Fax: 86-21-34204348

The authors declare that there is no conflict of interest.

Half-time Convergence Analysis. In this study, we calculated time-dependent cumulative averages of simulated average unsigned errors (AUE) of Cα chemical shifts as NMR observable. And using biphasic decay model to evaluate the convergence rate that simulated observables tend to balance. We focused on the slow stage and calculated the half-time of the slow stage. The fitting model of biphasic exponential decay for all IDPs is shown in Figure S35. The figure indicates that the two *ff03CMAP* force fields have smaller $\tau_2 \ln(2)$ (half-time of the slow stage) and lower N_0 (plateau) than other force fields, which suggested the efficient convergence for IDP.

The average half-time of simulated IDPs for six *ff03*-series force field is gathered in Table S23. It is obvious that the average half-time and standard deviation of *ff03CMAP* are smaller than others. Moreover, the plateaus of the Cα chemical shifts for *ff03CMAP* force fields are lower from the details of modeling parameters. These results suggested that *ff03CMAP* force fields are more efficient than other *ff03*-series force fields.

Definition of AAQAA3 Helicity. In this work, the definition of the helicity we calculated is from the *Best*'s work published in 2009.[1] The definition of a given residue is helical is that this residue is one of the residues in helical fragment. Helical fragment is defined as a fragment has at least three consecutive residues whose (φ,ψ) angles fall within the R_h boundaries (The R_h region of the (φ,ψ) map is defined more stringently as $\varphi \in [-100°, -30°]$ and $\psi \in [-67°, -7°]$).

Table S1. Simulation condition for all tested protein or peptide system.

System	Description	Length	Initial Structure	Simulation Temperature/ K	Ions	Number of Waters	Simulation Time/ns	Number of Tested Force Field	Number of Trajectories or Replicas
Peptide									
ALA5	A-A-A-A-A	5	Extended	300	None	1349-1359	200	6	5
Folded Protein									
GB3	Third Immunoglobulin Binding Domain of Protein G	56	PDB 1P7E	298	50mM NaCl	3318-3371	1000	6	1
BPTI	Free Bovine Pancreatic Trypsin Inhibitor	58	PDB 5PTI	309	None	4580-5453	1000	6	1
CspTm	Cold-shock Protein from the Hyperthermophilic Bacterium *Thermotoga maritima*	66	PDB 1G6P	303	150mM NaCl	4253-4313	1000	6	1
ubiquitin	Ubiquitin of Human	76	PDB 1UBQ	298	50mM NaCl	4589-4669	1000	6	1
SPR17	Chicken brain alpha spectrin repeat 17	118	PDB 1CUN	298	100mM NaCl	9447-9529	1000	6	1
Disordered Protein									
HEWL19	Hen Egg-White Lysozyme(19)	19	Extended	293	$2Cl^-$	11245-11425	200	6	5
RS	Phosphorylated SRSF1	24	Modeling	298	100mM NaCl	7277-8323	200	6	5
HIVRev	HIV-1 Rev ARM peptide	26	Modeling	283	$10Cl^-$	4617-4878	200	6	5
Aβ40	Amyloid-beta-peptides(1-40)	40	Modeling	277	100mM NaCl	8154-8285	200	7	5
Aβ42	Amyloid-beta-peptides(1-42)	42	PDB 1Z0Q	273	20mM NaCl	12264-12367	400	6	5
ACTR	Activation Domain of the Nuclear Hormone Receptor Coactivator	71	Modeling	304.15	50mM NaCl	12260-12600	200	7	5
IA3	An Aspartic Proteinase Inhibitor for *Saccharomyces cerevisiae*	76	Modeling	293	150mM NaCl	10854-11060	200	7	5
p53N	p53 N-terminal Transactivation Domain	93	PDB 1YCR	293	175mM NaCl	6128-7075	200	6	5
tauF4	Tau Protein Fragment	124	Modeling	293	25mM NaCl	11484-14126	200	6	5
Fast-Folding Protein									
CLN025	Chignolin, a 10-residue folded peptide designed by segment statistics	10	Extended	273.00-424.35	$2Na^+$	2194	400	2	32

AAQAA3	15-residue helix-forming peptide Ac-(AAQAA)3-NH2	15	Extended	278.00-391.21	None	3265	400	2	30
GB1	β-hairpin B1 domain of protein G	16	Extended	274.00-381.47	$3Na^+$	3502	600	2	30

Table S2. Experimental measurements used in this work.

Protein	Experimental Measurements
	Peptide
ALA5	Backbone Cα, Cβ, C, N, Hα and HN chemical shifts, backbone $^{1}J_{C\alpha N}$, $^{2}J_{C\alpha N}$, $^{3}J_{HNH\alpha}$, $^{3}J_{HNC\alpha}$, $^{3}J_{HNC\beta}$, $^{3}J_{H\alpha C}$ and $^{3}J_{HNC}$ scalar couplings[2]
	Folded Protein
GB3	Backbone Cα, Cβ, N, Hα and HN chemical shifts,[3] backbone $^{3}J_{HNH\alpha}$, $^{3}J_{HNC\beta}$ and $^{3}J_{H\alpha C}$ scalar couplings,[4] backbone amide S2 order parameters[5]
BPTI	Backbone Cα, Cβ, C, N, Hα and HN chemical shifts,[6] backbone $^{3}J_{HNH\alpha}$, $^{3}J_{HNC\beta}$, $^{3}J_{H\alpha C}$ and $^{3}J_{HNC}$ scalar couplings[7]
CspTm	Backbone Cα, Cβ, C, N, Hα and HN chemical shifts[8]
ubiquitin	Backbone Cα, Cβ, C, N, Hα and HN chemical shifts,[9] backbone $^{1}J_{H\alpha C\alpha}$, $^{1}J_{C\alpha C\beta}$, $^{1}J_{C\alpha N}$, $^{2}J_{C\alpha N}$, $^{3}J_{HNH\alpha}$, $^{3}J_{HNC\beta}$, $^{3}J_{H\alpha C}$ and $^{3}J_{HNC}$ scalar couplings,[10-12] side-chain $^{3}J_{CC\gamma}$ and $^{3}J_{NC\gamma}$ scalar couplings,[13] backbone N-HN, Cα-Hα, Cα-C, C-N and C-HN RDCs,[14-15] backbone amide S^2 order parameters,[16] side-chain methyl axis S^2 order parameters[17]
SPR17	Backbone Cα, Cβ, C, N, Hα and HN chemical shifts[18]
	Disordered Protein
HEWL19	Backbone Cα, N, Hα and HN chemical shifts[2]
RS	Backbone Cα and C chemical shifts, backbone $^{1}J_{C\alpha C\beta}$, $^{1}J_{H\alpha C\alpha}$ and $^{3}J_{HNH\alpha}$ scalar couplings, side-chain $^{3}J_{CC\gamma}$ and $^{3}J_{NC\gamma}$ scalar couplings, backbone N-HN, Cα-Hα and Cα-C RDCs[19], small-angle X-ray scattering curve, Rg[20]
HIVRev	Backbone Cα, Cβ, C, N, Hα and HN chemical shifts[21]
Aβ40	Backbone Cα, Cβ, N, Hα and HN chemical shifts,[22] backbone $^{1}J_{H\alpha C\alpha}$ $^{1}J_{C\alpha N}$, $^{2}J_{C\alpha N}$, $^{3}J_{HNH\alpha}$, $^{3}J_{H\alpha C}$ and $^{3}J_{CC}$ scalar couplings,[23] backbone N-HN RDC,[24] Rg[25]
Aβ42	Backbone Cα, Cβ, N, Hα and HN chemical shifts,[26] backbone $^{3}J_{HNH\alpha}$ scalar couplings,[23] backbone N-HN RDCs[24]
ACTR	Backbone Cα, Cβ, C, N, Hα and HN chemical shifts,[27] backbone N-HN RDCs,[28] Rg[29]
IA3	Backbone Cα, C, N, Hα and HN chemical shifts[30]
p53N	Backbone Cα, Cβ, C, N and HN chemical shifts[31]
tauF4	Backbone Cα, Cβ, N and HN chemical shifts[32]
	Fast-Folding Protein
CLN025	Temperature-dependent hairpin fraction[33]
AAQAA3	Temperature-dependent helical fraction[34]
GB1	Temperature-dependent native-state stability[35]

Table S3. FF score of six ff03-series force field for 15 tested system.

Force Field	*ff03/ TIP3P*	*ff03*/ TIP3P*	*ff03w/ TIP4P2005*	*ff03ws/ TIP4P2005*	*ff03CMAP/ TIP4PEw*	*ff03CMAP/ TIP4PD*
Peptide						
Ala5	1.950	1.468	1.564	1.599	1.178	1.155
Disordered Protein						
HEWL19	1.290	1.039	1.089	1.117	1.125	1.092
RS	4.453	1.657	1.600	1.454	1.140	1.105
HIVRev	1.761	1.763	1.677	1.208	1.244	1.295
Aβ40	2.016	1.756	1.872	1.758	1.124	1.001
Aβ42	2.106	1.866	1.972	1.858	1.184	1.021
ACTR	1.618	1.474	1.354	1.172	1.245	1.033
IA3	2.111	1.810	1.923	1.677	1.404	1.000
p53N	1.668	1.441	1.537	1.351	1.133	1.019
tauF4	1.587	1.590	1.384	1.301	1.226	1.000
Folded Protein						
GB3	1.185	1.212	1.246	1.209	1.001	1.099
BPTI	1.078	1.241	1.088	1.171	1.173	1.205
CspTm	1.376	1.674	1.718	1.663	1.000	1.123
ubiquitin	1.231	1.506	1.249	1.769	1.003	1.509
SPR17	1.026	1.041	1.052	1.219	1.019	1.220

Table S4. RMSD of secondary chemical shifts, J-coupling constants, S^2 parameter and FF score of **GB3** for six ff03-series force fields. Chemical shifts are in ppm and the scores are unitless, J-coupling constants are in Hz, and the scores and S^2 parameters are unitless.

	ff03/ TIP3P	***ff03*/ TIP3P***	***ff03w/ TIP4P2005***	***ff03ws/ TIP4P2005***	***ff03CMAP/ TIP4PEw***	***ff03CMAP/ TIP4PD***
Cα	0.599	0.628	0.591	0.596	0.529	0.684
Cβ	0.713	0.725	0.799	0.767	0.639	0.630
N	2.057	2.058	2.011	2.075	1.665	1.668
HA	0.149	0.166	0.176	0.154	0.112	0.147
HN	0.301	0.302	0.330	0.305	0.267	0.296
$^3J_{HNH\alpha}$	1.258	1.246	1.341	1.306	0.886	1.012
$^3J_{HNC}$	0.601	0.601	0.633	0.605	0.473	0.500
$^3J_{HNC\beta}$	0.419	0.437	0.477	0.465	0.374	0.430
S^2_{NH}	0.317	0.324	0.314	0.311	0.290	0.301
CS_{score}	1.192	1.237	1.281	1.222	1.003	1.144
Backbone ^3J	1.270	1.282	1.376	1.332	1.000	1.116
Backbone S^2	1.092	1.117	1.083	1.072	1.000	1.038
FF_{score}	**1.185**	**1.212**	**1.246**	**1.209**	**1.001**	**1.099**

Table S5. RMSD of secondary chemical shifts, J-coupling constants and FF score of **BPTI** for six ff03-series force fields. Chemical shifts are in ppm and the scores are unitless, J-coupling constants are in Hz, and the scores are unitless.

	ff03/ TIP3P	***ff03*/ TIP3P***	***ff03w/ TIP4P2005***	***ff03ws/ TIP4P2005***	***ff03CMAP/ TIP4PEw***	***ff03CMAP/ TIP4PD***
Cα	0.872	1.249	0.909	1.251	1.430	1.438
Cβ	1.770	1.892	1.723	1.818	1.683	1.839
C	0.784	1.044	0.795	0.854	0.910	1.114
N	2.171	3.022	2.454	3.192	3.213	3.224
HA	0.250	0.256	0.232	0.229	0.243	0.237
HN	0.417	0.615	0.467	0.590	0.653	0.669
$^3J_{HNH\alpha}$	1.639	2.044	1.665	1.822	1.500	1.542
$^3J_{H\alpha C}$	1.671	1.539	1.641	1.466	1.560	1.572
$^3J_{HNC}$	1.161	1.217	1.168	1.093	1.053	1.069
$^3J_{HNC\beta}$	1.458	1.353	1.392	1.372	1.274	1.221
CS_{score}	1.024	1.312	1.057	1.248	1.318	1.381
Backbone ^3J	1.132	1.169	1.120	1.094	1.027	1.029
FF_{score}	1.078	1.241	1.088	1.171	1.173	1.205

Table S6. RMSD of secondary chemical shifts and FF score of **CspTm** for six ff03-series force fields. Chemical shifts are in ppm and the scores are unitless.

	ff03/ TIP3P	***ff03*/ TIP3P***	***ff03w/ TIP4P2005***	***ff03ws/ TIP4P2005***	***ff03CMAP/ TIP4PEw***	***ff03CMAP/ TIP4PD***
Cα	1.012	1.156	1.007	1.134	0.836	0.859
Cβ	1.208	1.387	1.298	1.266	0.558	0.758
C	0.587	0.927	1.150	0.899	0.533	0.659
N	2.162	2.811	3.297	2.904	1.826	2.035
HA	0.296	0.296	0.299	0.301	0.248	0.249
HN	0.391	0.475	0.447	0.518	0.279	0.279
CS_{score}	1.376	1.674	1.718	1.663	1.000	1.123
FF_{score}	**1.376**	**1.674**	**1.718**	**1.663**	**1.000**	**1.123**

Table S7. RMSD of secondary chemical shifts, J-coupling constants, RDC, S^2 parameter and FF score of **ubiquitin** for six ff03-series force fields. Chemical shifts are in ppm, J-coupling constants and RDC are in Hz, and the scores and S^2 parameters are unitless.

	ff03/ TIP3P	***ff03*/ TIP3P***	***ff03w/ TIP4P2005***	***ff03ws/ TIP4P2005***	***ff03CMAP/ TIP4PEw***	***ff03CMAP/ TIP4PD***
Cα	0.481	0.716	0.507	0.723	0.485	0.575
Cβ	0.816	0.885	0.825	1.069	0.770	0.860
C	0.607	0.702	0.611	0.789	0.609	0.650
N	2.050	2.450	2.188	2.625	2.142	2.573
HA	0.145	0.185	0.141	0.234	0.106	0.165
HN	0.329	0.349	0.326	0.407	0.298	0.293
$^3J_{HNH\alpha}$	1.341	1.487	1.484	1.597	1.196	1.319
$^3J_{H\alpha C}$	0.684	0.725	0.623	0.986	0.410	0.609
$^3J_{HNC\beta}$	0.643	0.734	0.671	0.701	0.633	0.612
$^3J_{HNC}$	0.681	0.734	0.701	0.852	0.564	0.662
$^1J_{C\alpha N}$	0.465	0.567	0.494	0.588	0.415	0.469
$^1J_{H\alpha C\alpha}$	2.669	2.717	2.628	3.030	2.225	2.476
$^1J_{C\alpha C\beta}$	0.984	1.056	0.977	1.229	0.856	0.966
$^2J_{C\alpha N}$	0.464	0.555	0.437	0.682	0.361	0.477
$^2J_{CC\gamma}$	0.650	0.973	0.717	0.936	0.419	0.775
$^3J_{NC\gamma}$	0.490	0.592	0.501	0.557	0.428	0.496
S^2_{NH}	0.074	0.104	0.081	0.149	0.069	0.154
S^2_{axis}	0.279	0.260	0.247	0.289	0.174	0.279
RDC	0.174	0.249	0.187	0.325	0.166	0.222
CS_{score}	1.092	1.321	1.107	1.512	1.012	1.200
Backbone ^3J	1.225	1.359	1.228	1.562	1.004	1.182
Sidechain ^3J	1.348	1.853	1.440	1.768	1.000	1.504
Backbone S^2	1.070	1.510	1.175	2.156	1.000	2.226
Sidechain S^2	1.603	1.493	1.418	1.657	1.000	1.603
Backbone RDC	1.048	1.500	1.127	1.958	1.000	1.337
FF_{score}	**1.231**	**1.506**	**1.249**	**1.769**	**1.003**	**1.509**

Table S8. RMSD of secondary chemical shifts and FF score of **SPR17** for six ff03-series force fields. Chemical shifts are in ppm and the scores are unitless.

	ff03/ TIP3P	***ff03*/ TIP3P***	***ff03w/ TIP4P2005***	***ff03ws/ TIP4P2005***	***ff03CMAP/ TIP4PEw***	***ff03CMAP/ TIP4PD***
Cα	0.900	0.936	0.970	1.209	0.906	1.220
Cβ	0.702	0.754	0.733	0.887	0.716	0.814
C	0.985	0.984	0.952	1.253	0.987	1.231
N	1.852	1.858	1.774	2.026	1.858	2.306
HA	0.209	0.206	0.225	0.227	0.201	0.217
HN	0.442	0.438	0.457	0.477	0.426	0.484
CS_{score}	1.026	1.041	1.052	1.219	1.019	1.220
FF_{score}	**1.026**	**1.041**	**1.052**	**1.219**	**1.019**	**1.220**

Table S9. RMSD of secondary chemical shifts and FF score of **HEWL19** for six ff03-series force fields. Chemical shifts are in ppm and the scores are unitless.

	ff03/ TIP3P	***ff03*/ TIP3P***	***ff03w/ TIP4P2005***	***ff03ws/ TIP4P2005***	***ff03CMAP/ TIP4PEw***	***ff03CMAP/ TIP4PD***
Cα	1.516	1.215	1.184	1.175	1.189	1.158
N	1.754	1.393	1.481	1.259	1.394	1.267
Hα	0.206	0.181	0.191	0.199	0.187	0.194
HN	0.241	0.182	0.201	0.247	0.243	0.235
CS_{score}	1.290	1.039	1.089	1.117	1.125	1.092
FF_{score}	**1.290**	**1.039**	**1.089**	**1.117**	**1.125**	**1.092**

Table S10. RMSD of secondary chemical shifts, J-coupling constants, RDC and FF score of **RS** for six ff03-series force fields. Chemical shifts are in ppm, J-coupling constants and RDC are in Hz and the scores are unitless.

	ff03/ TIP3P	***ff03*/ TIP3P***	***ff03w/ TIP4P2005***	***ff03ws/ TIP4P2005***	***ff03CMAP/ TIP4PEw***	***ff03CMAP/ TIP4PD***
Cα	1.813	0.502	0.484	0.385	0.239	0.193
C	1.199	0.333	0.296	0.307	0.354	0.373
$^{3}J_{HNH\alpha}$	1.777	0.987	0.974	0.981	0.407	0.491
$^{1}J_{C\alpha C\beta}$	1.625	1.407	1.420	1.438	1.084	1.195
$^{1}J_{H\alpha C\alpha}$	4.190	2.462	2.511	2.395	1.774	1.824
$^{3}J_{CC\gamma}$	0.302	0.314	0.271	0.278	0.330	0.311
$^{3}J_{NC\gamma}$	0.386	0.254	0.272	0.233	0.230	0.217
RDC	1.425	0.908	0.939	0.841	0.788	0.716
CS_{score}	6.720	1.862	1.753	1.514	1.217	1.128
NMR_{score}	2.186	1.451	1.448	1.394	1.063	1.081
FF_{score}	**4.453**	**1.657**	**1.600**	**1.454**	**1.140**	**1.105**

Table S11. RMSD of secondary chemical shifts and FF score of **HIVRev** for six ff03-series force fields. Chemical shifts are in ppm and the scores are unitless.

	ff03/ TIP3P	***ff03*/ TIP3P***	***ff03w/ TIP4P2005***	***ff03ws/ TIP4P2005***	***ff03CMAP/ TIP4PEw***	***ff03CMAP/ TIP4PD***
Cα	1.192	0.909	1.043	0.401	0.522	0.600
Cβ	0.337	0.721	0.433	0.609	0.491	0.545
C	0.596	1.200	0.636	0.693	0.801	0.879
N	2.212	1.274	1.957	1.193	1.283	1.024
Hα	0.112	0.090	0.100	0.062	0.061	0.073
HN	0.345	0.309	0.333	0.235	0.237	0.214
CS_{score}	1.761	1.763	1.677	1.208	1.244	1.295
FF_{score}	**1.761**	**1.763**	**1.677**	**1.208**	**1.244**	**1.295**

Table S12. RMSD of secondary chemical shifts, J-coupling constants, RDC and FF score of **Aβ40** for seven ff03-series force fields. Chemical shifts are in ppm, J-coupling constants and RDC are in Hz and the scores are unitless.

	ff03/ TIP3P	***ff03*/ TIP3P***	***ff03w/ TIP4P2005***	***ff03ws/ TIP4P2005***	***ff03CMAP/ TIP4PEw***	***ff03CMAP/ TIP4PD***	***ff03/ TIP4PD***
Cα	1.093	0.943	1.026	0.940	0.445	0.426	0.905
Cβ	0.648	0.512	0.547	0.621	0.422	0.398	0.657
N	3.324	2.873	2.962	2.580	1.539	1.291	2.751
Hα	0.125	0.101	0.122	0.108	0.087	0.087	0.105
HN	0.404	0.365	0.382	0.375	0.284	0.259	0.352
$^{3}J_{HNH\alpha}$	1.320	1.261	1.252	0.983	0.563	0.513	1.114
$^{3}J_{H\alpha C}$	0.949	0.987	0.978	1.017	0.634	0.407	1.003
$^{3}J_{CC}$	0.391	0.322	0.375	0.375	0.161	0.135	0.374
$^{1}J_{C\alpha N}$	0.585	0.469	0.524	0.559	0.474	0.431	0.548
$^{1}J_{H\alpha C\alpha}$	2.835	2.545	2.607	2.460	1.550	1.383	2.311
$^{2}J_{C\alpha N}$	1.254	0.936	1.090	0.840	0.603	0.561	0.972
RDC	0.790	0.783	0.722	0.721	0.757	0.719	0.728
CS_{score}	1.955	1.660	1.791	1.692	1.078	1.002	1.696
NMR_{score}	2.077	1.851	1.953	1.825	1.171	1.000	1.870
FF_{score}	**2.016**	**1.756**	**1.872**	**1.758**	**1.124**	**1.001**	**1.783**

Table S13. RMSD of secondary chemical shifts, J-coupling constants, RDC and FF score of **Aβ42** for six ff03-series force fields. Chemical shifts are in ppm, J-coupling constants and RDC are in Hz and the scores are unitless.

	ff03/ TIP3P	***ff03*/ TIP3P***	***ff03w/ TIP4P2005***	***ff03ws/ TIP4P2005***	***ff03CMAP/ TIP4PEw***	***ff03CMAP/ TIP4PD***
Cα	1.793	1.398	1.554	1.421	0.747	0.383
Cβ	0.622	0.674	0.649	0.658	0.427	0.378
N	3.278	2.931	3.150	3.029	1.965	1.362
Hα	0.190	0.198	0.194	0.200	0.199	0.207
HN	0.287	0.293	0.297	0.288	0.229	0.228
$^{3}J_{HNH\alpha}$	1.748	1.446	1.595	1.419	0.610	0.586
RDC	0.729	0.720	0.699	0.710	0.743	0.733
CS_{score}	2.198	1.982	2.082	1.997	1.315	1.018
NMR_{score}	2.014	1.750	1.862	1.719	1.052	1.024
FF_{score}	**2.106**	**1.866**	**1.972**	**1.858**	**1.184**	**1.021**

Table S14. RMSD of secondary chemical shifts, RDC and FF score of **ACTR** for seven ff03-series force fields. Chemical shifts are in ppm, RDC are in Hz and the scores are unitless.

	ff03/ TIP3P	***ff03*/ TIP3P***	***ff03w/ TIP4P2005***	***ff03ws/ TIP4P2005***	***ff03CMAP/ TIP4PEw***	***ff03CMAP/ TIP4PD***	***ff03/ TIP4PD***
Cα	1.420	1.233	1.066	0.841	0.708	0.469	1.049
Cβ	0.524	0.461	0.470	0.376	0.525	0.316	0.449
C	1.107	0.901	0.768	0.622	0.522	0.531	0.758
N	2.323	2.141	1.962	1.467	1.566	1.134	2.049
HN	0.268	0.252	0.234	0.203	0.201	0.162	0.248
RDC	0.767	0.742	0.694	0.676	0.766	0.719	0.700
NMR_{score}	1.135	1.098	1.027	1.000	1.133	1.064	1.036
CS_{score}	2.101	1.851	1.681	1.344	1.358	1.003	1.689
FF_{score}	**1.618**	**1.474**	**1.354**	**1.172**	**1.245**	**1.033**	**1.362**

Table S15. RMSD of secondary chemical shifts and FF score of **IA3** for seven ff03-series force fields. Chemical shifts are in ppm and the scores are unitless.

	ff03/ TIP3P	***ff03*/ TIP3P***	***ff03w/ TIP4P2005***	***ff03ws/ TIP4P2005***	***ff03CMAP/ TIP4PEw***	***ff03CMAP/ TIP4PD***	***ff03/ TIP4PD***
Cα	1.841	1.505	1.608	1.416	1.060	0.658	1.464
C	1.269	0.993	1.092	1.015	0.740	0.625	0.965
N	2.785	2.661	2.818	2.471	2.114	1.430	2.612
Hα	0.197	0.167	0.162	0.128	0.150	0.103	0.162
HN	0.403	0.365	0.406	0.353	0.278	0.216	0.365
CS_{score}	2.111	1.810	1.923	1.677	1.404	1.000	1.773
FF_{score}	**2.111**	**1.810**	**1.923**	**1.677**	**1.404**	**1.000**	**1.773**

Table S16. RMSD of secondary chemical shifts and FF score of **p53N** for six ff03-series force fields. Chemical shifts are in ppm and the scores are unitless.

	ff03/ TIP3P	***ff03*/ TIP3P***	***ff03w/ TIP4P2005***	***ff03ws/ TIP4P2005***	***ff03CMAP/ TIP4PEw***	***ff03CMAP/ TIP4PD***
Cα	1.295	0.994	1.081	0.957	0.512	0.561
Cβ	0.628	0.603	0.603	0.554	0.616	0.484
C	0.651	0.589	0.628	0.551	0.557	0.511
N	2.629	2.347	2.518	2.048	1.876	1.457
HN	0.364	0.318	0.348	0.318	0.257	0.254
CS_{score}	1.668	1.441	1.537	1.351	1.133	1.019
FF_{score}	**1.668**	**1.441**	**1.537**	**1.351**	**1.133**	**1.019**

Table S17. RMSD of secondary chemical shifts and FF score of **tauF4** for six ff03-series force fields. Chemical shifts are in ppm and the scores are unitless.

	ff03/ TIP3P	***ff03*/ TIP3P***	***ff03w/ TIP4P2005***	***ff03ws/ TIP4P2005***	***ff03CMAP/ TIP4PEw***	***ff03CMAP/ TIP4PD***
Cα	1.034	0.978	0.770	0.779	0.822	0.722
Cβ	0.685	0.807	0.713	0.632	0.556	0.507
N	2.966	2.739	2.516	2.401	2.023	1.488
HN	0.339	0.339	0.296	0.273	0.282	0.216
CS_{score}	1.587	1.590	1.384	1.301	1.226	1.000
FF_{score}	**1.587**	**1.590**	**1.384**	**1.301**	**1.226**	**1.000**

Table S18. Side-chain $^{3}J_{CC\gamma}$ coupling constant of ubiquitin for six ff03-series force fields. J-coupling constants are in Hz.

	Exp.	***ff03/ TIP3P***	***ff03*/ TIP3P***	***ff03w/ TIP4P2005***	***ff03ws/ TIP4P2005***	***ff03CMAP/ TIP4PEw***	***ff03CMAP/ TIP4PD***
I3γ2	3.68	3.681	3.051	3.505	3.036	3.885	1.543
V5γ1	0.00	0.687	0.893	0.709	0.751	0.751	0.710
V5γ2	3.66	2.986	2.539	2.974	3.553	3.804	3.500
T7γ2	2.67	2.628	3.734	3.526	3.003	3.437	3.827
T9γ2	3.00	3.650	3.379	3.562	3.519	3.684	3.330
T12γ2	0.39	0.811	0.763	0.807	0.916	0.717	0.919
I13γ2	1.71	3.500	3.698	3.561	3.250	2.269	2.930
T14γ2	0.76	2.216	2.100	1.968	1.772	1.082	1.250
V17γ1	3.93	3.241	3.186	2.879	2.976	3.530	2.939
V17γ2	0.96	0.878	0.963	0.950	0.643	0.976	1.419
T22γ2	3.39	3.761	3.642	3.555	2.781	3.756	3.027
I23γ2	0.94	0.835	0.829	0.857	1.298	0.855	1.597
V26γ1	0.82	0.855	0.836	0.835	1.504	0.704	0.776
V26γ2	4.18	3.724	3.639	3.700	2.789	3.788	3.491
I30γ2	0.96	0.919	2.400	0.961	1.968	0.901	0.903
I36γ2	0.71	1.025	2.201	1.130	1.825	1.097	0.602
I44γ2	0.80	1.317	1.831	1.552	3.147	0.792	0.905
T55γ2	3.02	3.633	3.657	3.627	3.264	3.782	3.106
I61γ2	0.98	0.939	0.881	0.833	1.339	0.770	0.893
V70γ2	2.43	2.278	0.809	1.617	1.657	2.677	1.344
RMSD	**-**	**0.650**	**0.973**	**0.717**	**0.936**	**0.419**	**0.775**

Table S19. Side-chain $^{3}J_{NC\gamma}$ coupling constant of ubiquitin for six ff03-series force fields. J-coupling constants are in Hz.

	Exp.	***ff03/ TIP3P***	***ff03*/ TIP3P***	***ff03w/ TIP4P2005***	***ff03ws/ TIP4P2005***	***ff03CMAP/ TIP4PEw***	***ff03CMAP/ TIP4PD***
I3γ2	0.39	0.399	0.443	0.414	0.435	0.392	0.962
V5γ1	1.83	1.782	1.525	1.772	2.091	2.224	2.062
V5γ2	0.46	0.987	1.102	0.980	0.657	0.515	0.703
T7γ2	1.02	1.089	0.545	0.620	0.682	0.718	0.478
T9γ2	0.81	0.502	0.643	0.548	0.536	0.486	0.668
T12γ2	1.61	2.120	2.159	2.069	2.043	2.197	2.051
I13γ2	1.44	0.611	0.477	0.568	0.726	1.329	0.947
T14γ2	1.50	0.798	1.008	0.992	0.774	1.690	1.776
V17γ1	0.25	0.579	0.624	0.620	0.452	0.630	0.881
V17γ2	0.68	0.674	0.662	0.834	0.938	0.469	0.559
T22γ2	0.75	0.487	0.553	0.523	0.621	0.540	0.475
I23γ2	2.11	1.343	0.836	1.048	1.179	0.747	1.159
V26γ1	2.16	2.156	2.132	2.149	1.645	2.223	2.039
V26γ2	0.62	0.495	0.562	0.523	0.632	0.561	0.666
I30γ2	2.10	2.223	1.062	2.190	0.891	2.232	2.227
I36γ2	2.08	0.657	0.752	0.728	1.189	1.475	0.723
I44γ2	1.62	1.887	1.403	1.745	0.729	2.169	2.128
T55γ2	0.82	0.541	0.537	0.548	0.741	0.474	0.535
I61γ2	2.15	2.140	2.051	2.207	1.545	2.245	1.951
V70γ2	0.50	0.556	0.556	0.543	0.609	0.510	0.568
RMSD	**-**	**0.490**	**0.592**	**0.501**	**0.557**	**0.428**	**0.496**

Table S20. Side-chain methyl axis order parameters of ubiquitin for six ff03-series force fields. Order parameters are in unitless.

	Exp.	***ff03/ TIP3P***	***ff03*/ TIP3P***	***ff03w/ TIP4P2005***	***ff03ws/ TIP4P2005***	***ff03CMAP/ TIP4PEw***	***ff03CMAP/ TIP4PD***
I3γ	0.98	0.359	0.742	0.820	0.761	0.916	0.359
I3δ	0.75	0.345	0.532	0.632	0.631	0.616	0.345
V5γ1	0.91	0.676	0.446	0.629	0.748	0.852	0.676
V5γ2	0.88	0.695	0.443	0.647	0.742	0.844	0.695
T7γ	0.75	0.767	0.751	0.652	0.449	0.602	0.767
L8δ1	0.27	0.196	0.331	0.253	0.340	0.292	0.196
L8δ2	0.21	0.176	0.347	0.225	0.361	0.217	0.176
T9γ	0.64	0.452	0.487	0.564	0.511	0.531	0.452
T12γ	0.93	0.680	0.774	0.660	0.617	0.816	0.680
I13γ	0.56	0.587	0.762	0.702	0.592	0.387	0.587
I13δ	0.55	0.546	0.634	0.648	0.548	0.345	0.546
T14γ	0.78	0.401	0.206	0.207	0.305	0.426	0.401
L15δ1	0.58	0.484	0.251	0.180	0.447	0.398	0.484
L15δ2	0.62	0.442	0.292	0.181	0.419	0.410	0.442
V17γ1	0.89	0.393	0.534	0.364	0.512	0.680	0.393
V17γ2	0.89	0.391	0.528	0.393	0.547	0.682	0.391
T22γ	0.95	0.547	0.798	0.711	0.533	0.841	0.547
I23γ	0.95	0.595	0.795	0.785	0.578	0.756	0.595
I23δ	0.51	0.547	0.742	0.778	0.340	0.802	0.547
V26γ1	0.86	0.676	0.729	0.735	0.530	0.867	0.676
V26γ2	0.99	0.675	0.724	0.740	0.531	0.870	0.675
I30γ	0.93	0.923	0.664	0.886	0.654	0.928	0.923
I30δ	0.77	0.795	0.585	0.699	0.443	0.586	0.795
I36γ	0.83	0.793	0.514	0.601	0.421	0.427	0.793
I36δ	0.58	0.665	0.495	0.540	0.285	0.466	0.665
L43δ1	0.55	0.389	0.372	0.332	0.522	0.351	0.389
L43δ2	0.61	0.333	0.348	0.306	0.522	0.335	0.333
I44γ	0.71	0.750	0.446	0.470	0.714	0.792	0.750
I44δ	0.31	0.289	0.336	0.225	0.613	0.182	0.289
A46β	0.95	0.643	0.619	0.658	0.712	0.687	0.643
L50δ1	0.89	0.252	0.459	0.586	0.270	0.718	0.252
L50δ2	0.86	0.275	0.440	0.553	0.289	0.690	0.275
T55γ	0.93	0.606	0.733	0.711	0.482	0.824	0.606
L56δ1	0.60	0.355	0.353	0.368	0.492	0.393	0.355
L56δ2	0.62	0.355	0.384	0.377	0.487	0.398	0.355
I61γ	0.95	0.516	0.659	0.819	0.341	0.850	0.516
I61δ	0.56	0.270	0.220	0.194	0.199	0.269	0.270
L67δ1	0.30	0.153	0.284	0.316	0.473	0.305	0.153
L67δ2	0.29	0.234	0.259	0.300	0.454	0.351	0.234
L69δ2	0.55	0.844	0.372	0.841	0.514	0.784	0.844
V70γ2	0.35	0.443	0.648	0.375	0.446	0.352	0.443

L71δ1	0.29	0.282	0.174	0.198	0.157	0.273	0.282
L73δ1	0.19	0.142	0.082	0.083	0.118	0.069	0.142
L73δ2	0.17	0.211	0.128	0.128	0.145	0.109	0.211
RMSD	**-**	**0.279**	**0.260**	**0.247**	**0.289**	**0.174**	**0.279**

Table S21. Side-chain $^{3}J_{CC\gamma}$ coupling constant of RS for six ff03-series force fields. J-coupling constants are in Hz.

	Exp.	***ff03/ TIP3P***	***ff03*/ TIP3P***	***ff03w/ TIP4P2005***	***ff03ws/ TIP4P2005***	***ff03CMAP/ TIP4PEw***	***ff03CMAP/ TIP4PD***
R9γ	2.45	2.006	2.276	2.165	2.358	2.471	2.396
R11γ	2.17	2.143	2.141	2.355	2.193	2.609	2.648
R13γ	2.53	2.034	2.203	2.225	2.126	2.284	2.470
R15γ	1.89	2.045	2.327	2.108	2.272	2.389	2.323
R17γ	1.89	2.027	2.051	2.211	2.265	2.477	2.346
R19γ	2.42	2.415	2.029	2.116	2.138	2.338	2.399
R21γ	2.17	2.057	1.808	2.024	2.013	2.271	2.351
R23γ	2.56	2.082	2.176	2.221	2.323	2.647	2.229
RMSD	**-**	**0.302**	**0.314**	**0.271**	**0.278**	**0.330**	**0.311**

Table S22. Side-chain $^{3}J_{NC\gamma}$ coupling constant of RS for six ff03-series force fields. J-coupling constants are in Hz.

	Exp.	***ff03/ TIP3P***	***ff03*/ TIP3P***	***ff03w/ TIP4P2005***	***ff03ws/ TIP4P2005***	***ff03CMAP/ TIP4PEw***	***ff03CMAP/ TIP4PD***
R9γ	1.19	1.229	1.042	1.036	1.042	0.956	0.951
R11γ	0.98	1.301	1.024	0.941	0.962	0.988	0.894
R13γ	0.77	1.356	1.014	1.025	1.027	0.960	0.921
R15γ	0.77	1.301	0.907	1.107	0.948	0.982	0.917
R17γ	0.76	1.168	1.088	1.144	0.963	0.920	0.910
R19γ	0.79	0.989	1.014	1.028	1.006	0.989	1.010
R21γ	0.68	1.128	1.161	1.031	1.086	1.035	0.999
R23γ	0.63	0.870	0.793	0.880	0.879	0.941	0.937
RMSD	**-**	**0.386**	**0.254**	**0.272**	**0.233**	**0.230**	**0.217**

Table S23. Average half-time of IDPs simulation for six ff03-series force fields [a]

Force Field	*ff03/ TIP3P*	*ff03*/ TIP3P*	*ff03w/ TIP4P2005*	*ff03ws/ TIP4P2005*	*ff03CMAP/ TIP4PEw*	*ff03CMAP/ TIP4PD*
Half-time ±std/ns	271±319	331±765	111±86	977±2616	62±50	35±14

[a]. We calculated the average half-time for IDPs that the R2 of fitted model is larger than 0.90. Here std. means standard deviation.

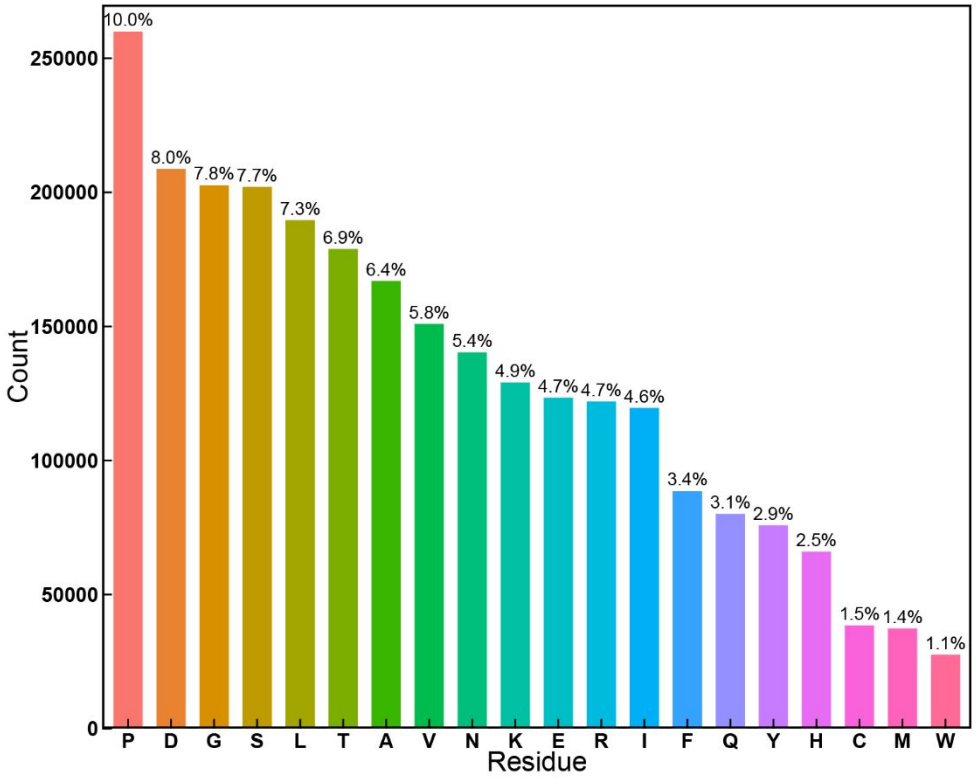

Figure S1. Count of amino acids in coil database.

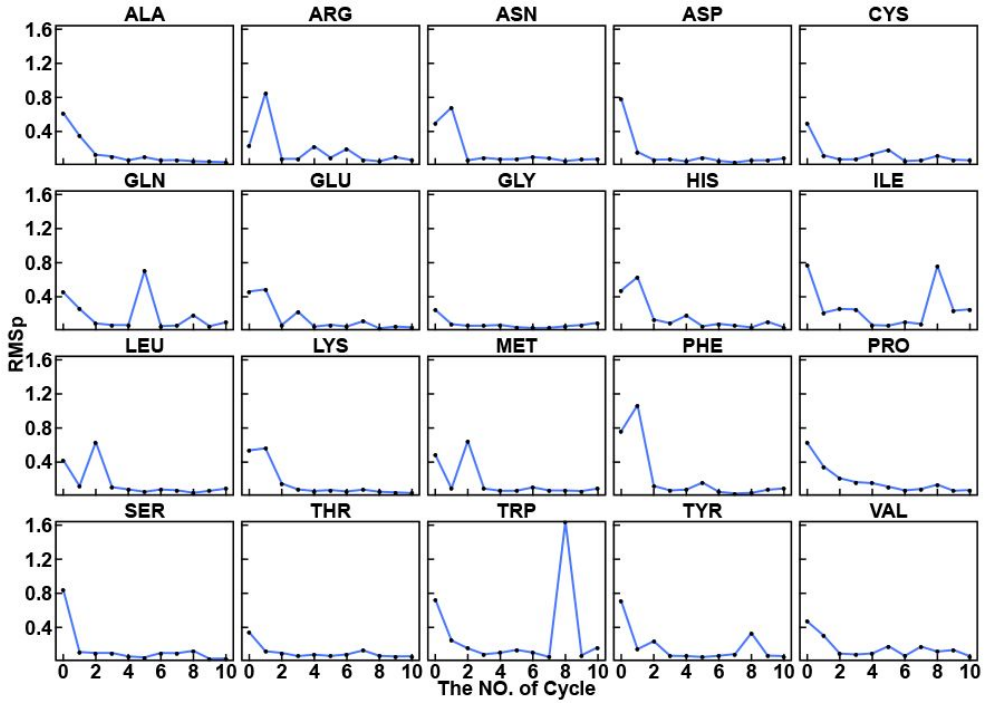

Figure S2. RMSp between simulation and benchmark for CMAP optimization of 20 amino acids.

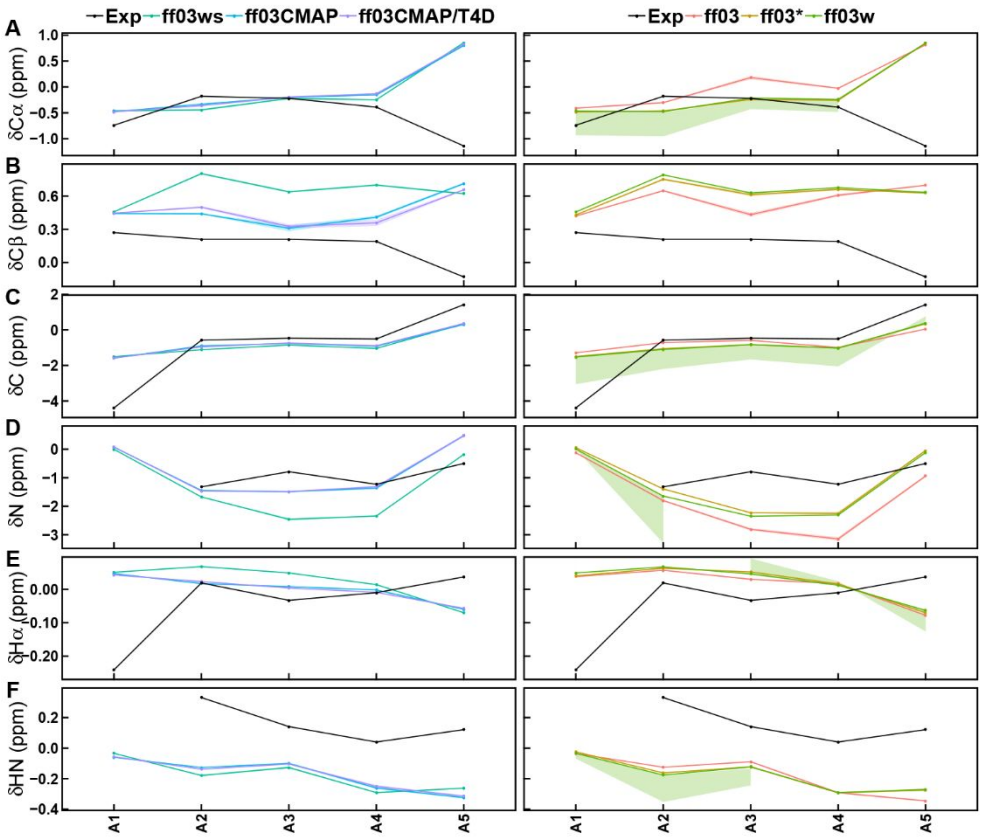

Figure S3. Secondary chemical shifts of simulation and experimental data for Ala_5. Here ff03CMAP means ff03CMAP force field with TIP4P-Ew water model, ff03CMAP/T4D means ff03CMAP force field with TIP4P-D water model and ff03/T4D means ff03 force field with TIP4P-D water model. Simulated and experimental secondary chemical shifts for (A) Cα, (B) Cβ, (C) C, (D) N, (E) Hα and (F) HN. Simulated values are shown for ff03 (red), ff03* (brown), ff03w (light green), ff03ws (cyan), ff03CMAP (blue), ff03CMAP/T4D (violet) and ff03/T4D (mauve). Experimental values are displayed as black lines. The shadow means the stand error of mean.

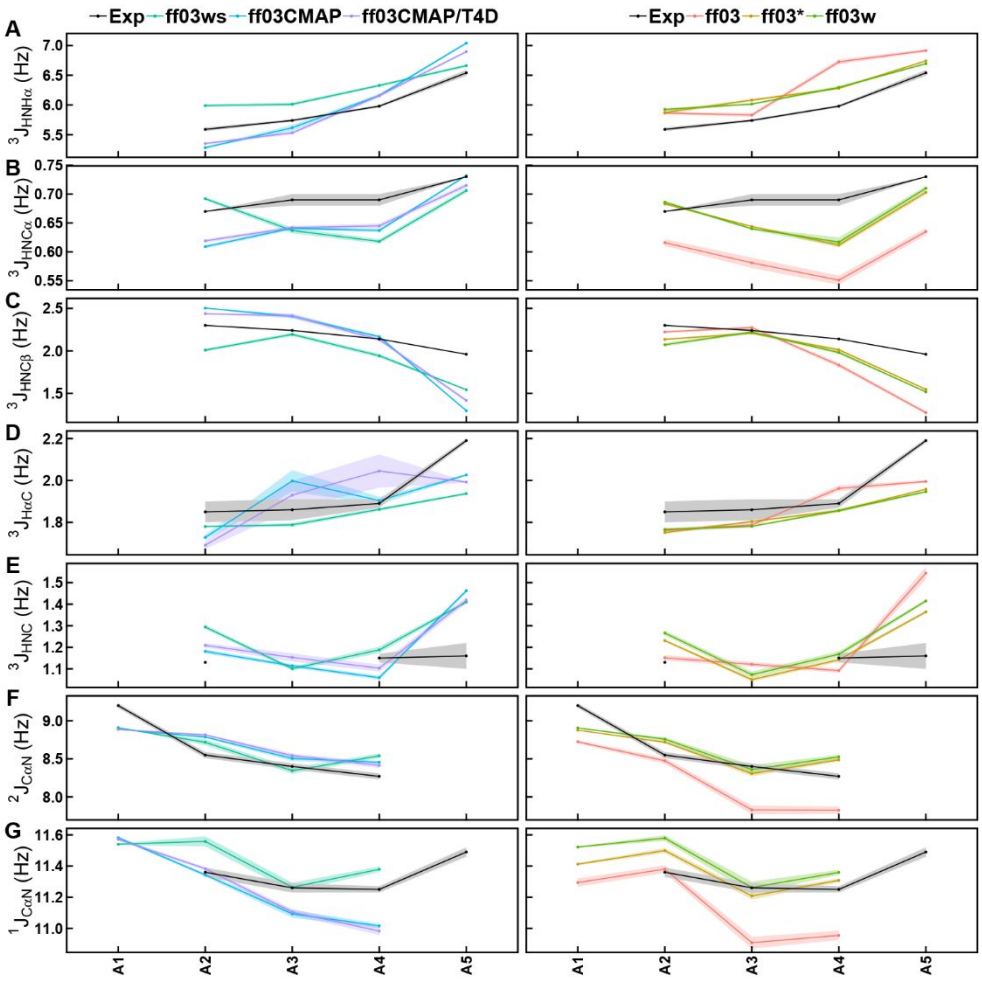

Figure S4. Scalar coupling constants of simulation and experimental data for Ala_5. Simulated and experimental scalar coupling constants for (A) $^3J_{HNH\alpha}$, (B) $^3J_{HNC\alpha}$, (C) $^3J_{HNC\beta}$, (D) $^3J_{H\alpha C}$, (E) $^3J_{HNC}$, (F) $^2J_{C\alpha N}$ and (G) $^1J_{C\alpha N}$.

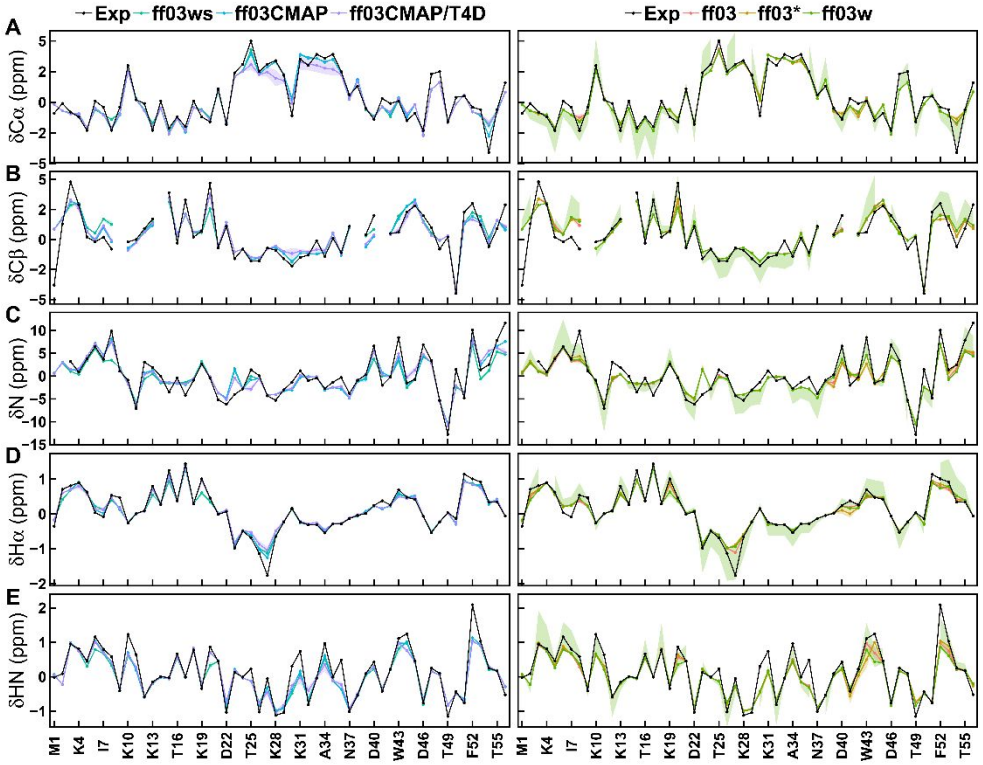

Figure S5. Secondary chemical shifts of simulation and experimental data for GB3. Simulated and experimental secondary chemical shifts for (A) Cα, (B) Cβ, (C) N, (D) Hα and (E) HN.

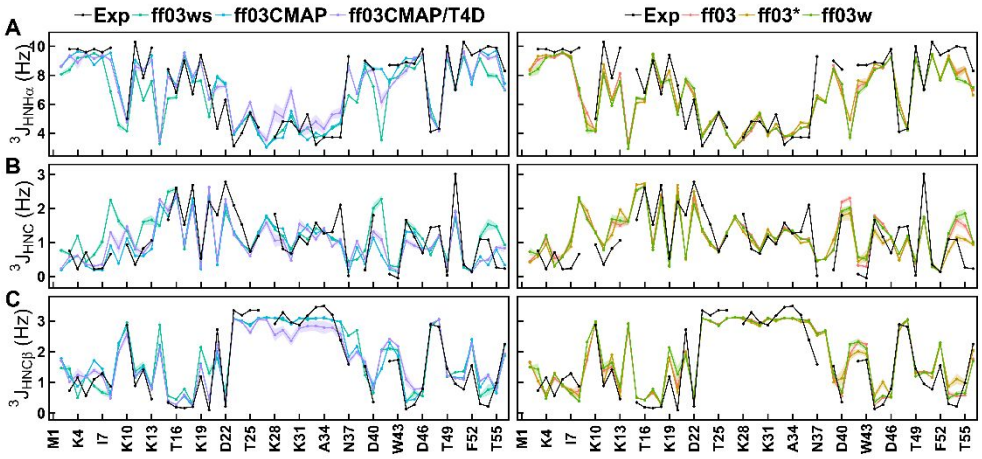

Figure S6. Scalar coupling constants of simulation and experimental data for GB3. Simulated and experimental scalar coupling constants for (A) $^3J_{HNH\alpha}$, (B) $^3J_{HNC}$ and (C) $^3J_{HNC\beta}$.

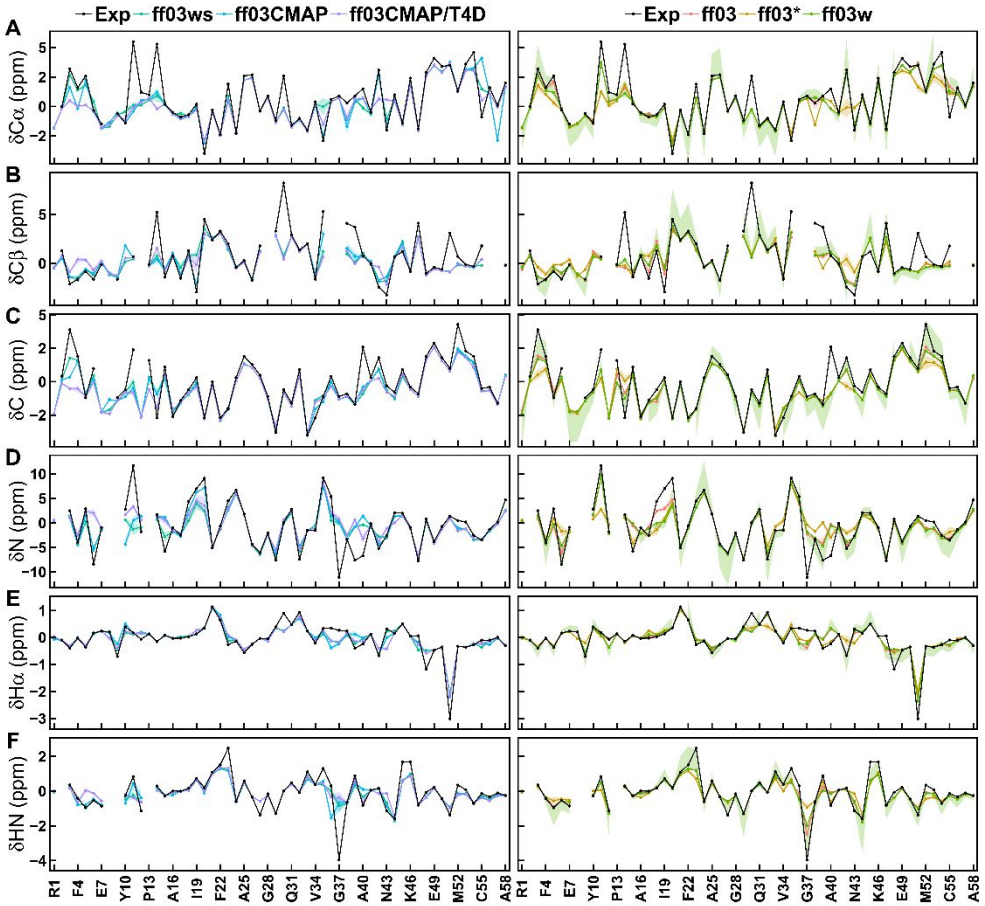

Figure S7. Secondary chemical shifts of simulation and experimental data for BPTI. Simulated and experimental secondary chemical shifts for (A) Cα, (B) Cβ, (C) C, (D) N, (E) Hα and (F) HN.

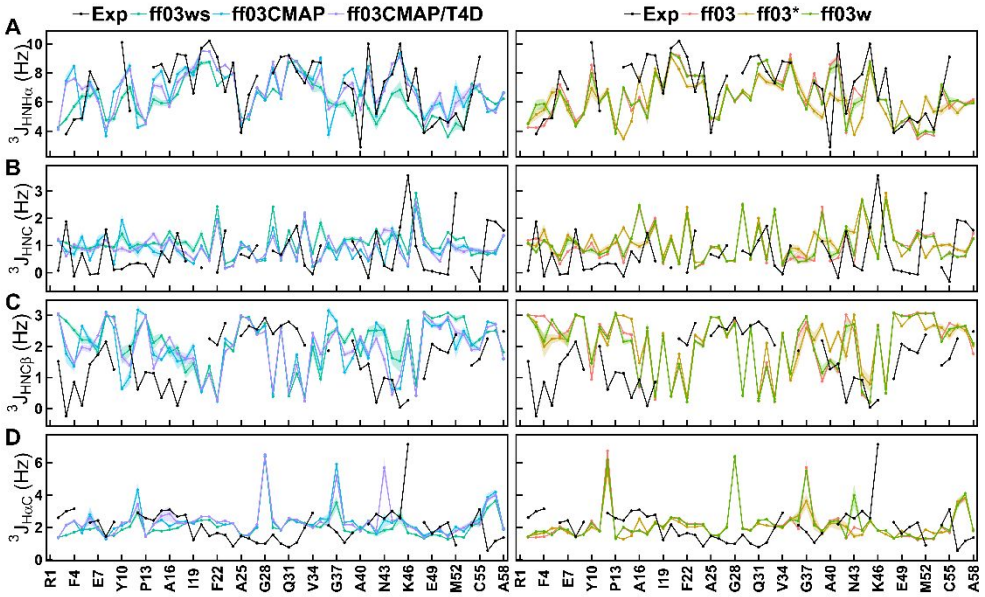

Figure S8. Scalar coupling constants of simulation and experimental data for BPTI. Simulated and experimental scalar coupling constants for (A) $^3J_{HNH\alpha}$, (B) $^3J_{HNC}$, (C) $^3J_{HNC\beta}$ and (D) $^3J_{H\alpha C}$.

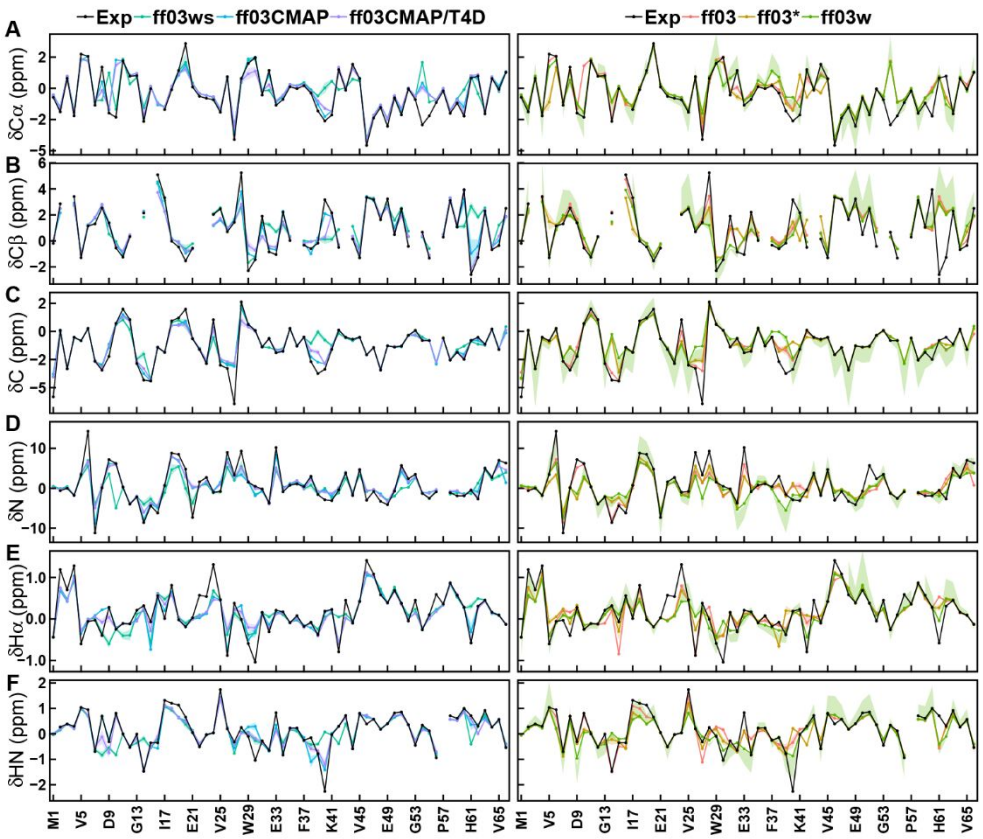

Figure S9. Secondary chemical shifts of simulation and experimental data for CspTm. Simulated and experimental secondary chemical shifts for (A) Cα, (B) Cβ, (C) C, (D) N, (E) Hα and (F) HN.

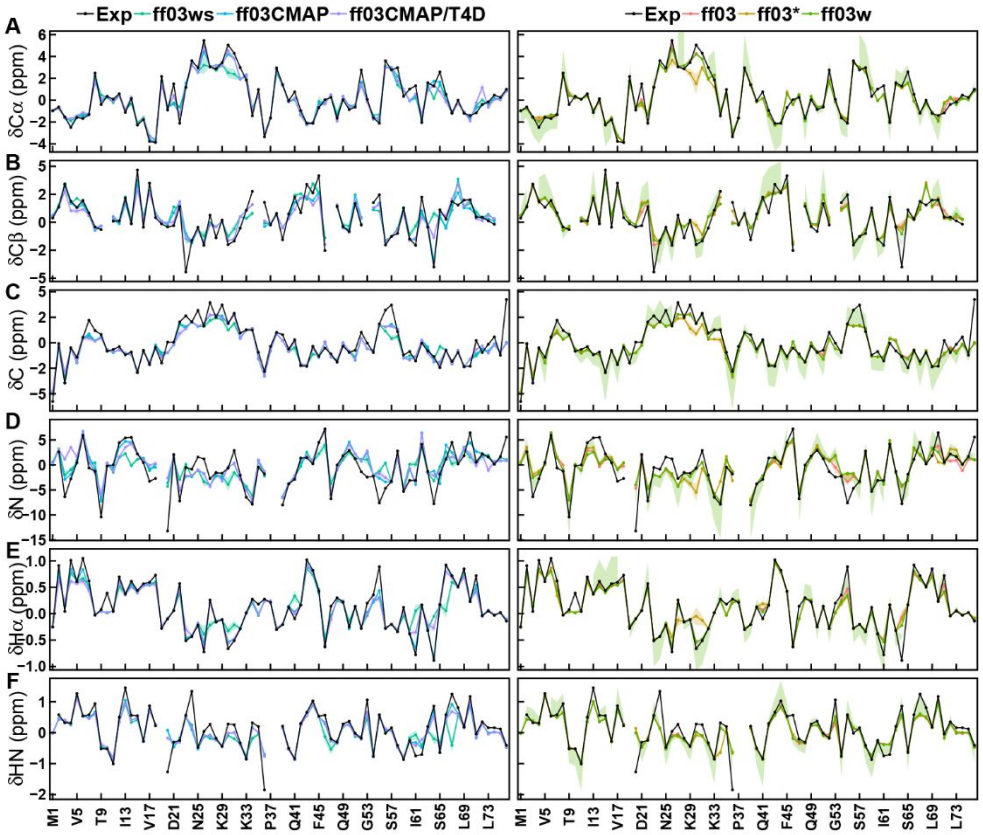

Figure S10. Secondary chemical shifts of simulation and experimental data for ubiquitin. Simulated and experimental secondary chemical shifts for (A) Cα, (B) Cβ, (C) C, (D) N, (E) Hα and (F) HN.

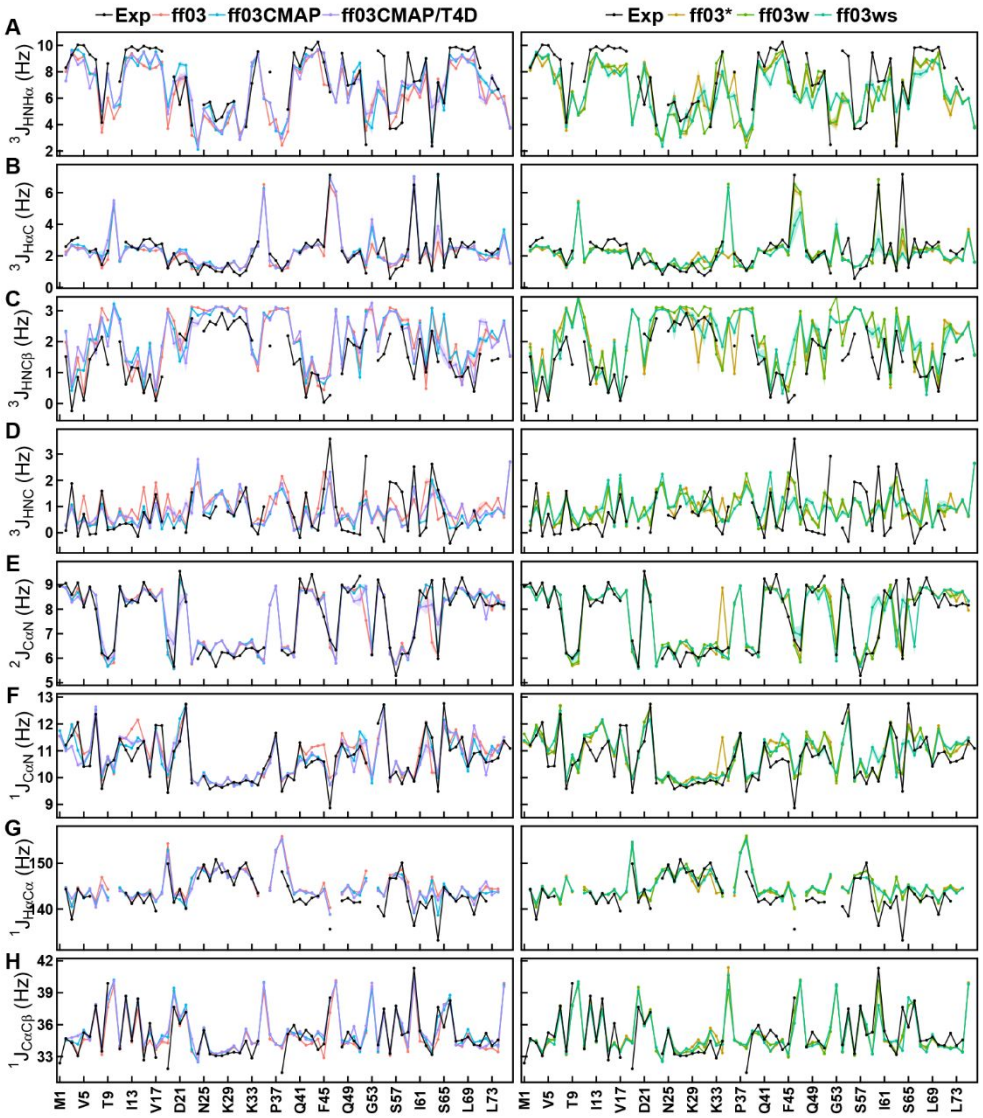

Figure S11. Scalar coupling constants of simulation and experimental data for ubiquitin. Simulated and experimental scalar coupling constants for (A) $^3J_{HNH\alpha}$, (B) $^3J_{H\alpha C}$, (C) $^3J_{HNC\beta}$, (D) $^3J_{HNC}$, (E) $^2J_{C\alpha N}$, (F) $^1J_{C\alpha N}$, (G) $^1J_{H\alpha C\alpha}$ and (H) $^1J_{C\alpha C\beta}$.

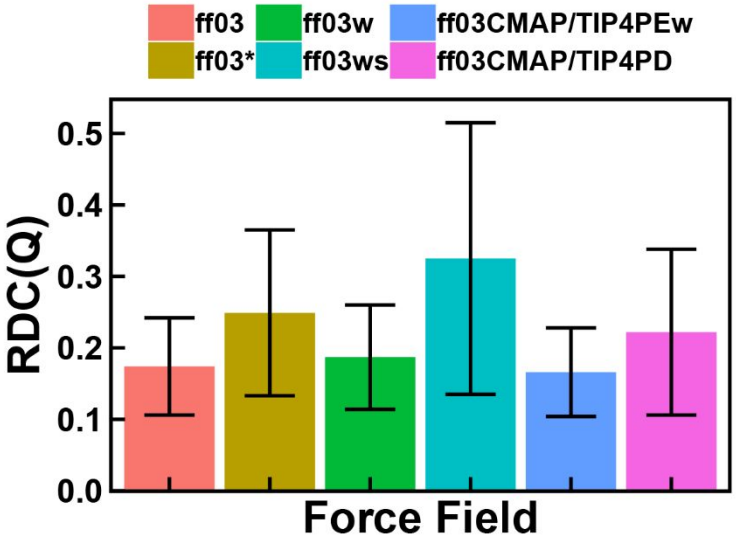

Figure S12. Backbone RDC of simulation of six ff03-series force fields for ubiquitin. Error bar means the standard deviation of calculation.

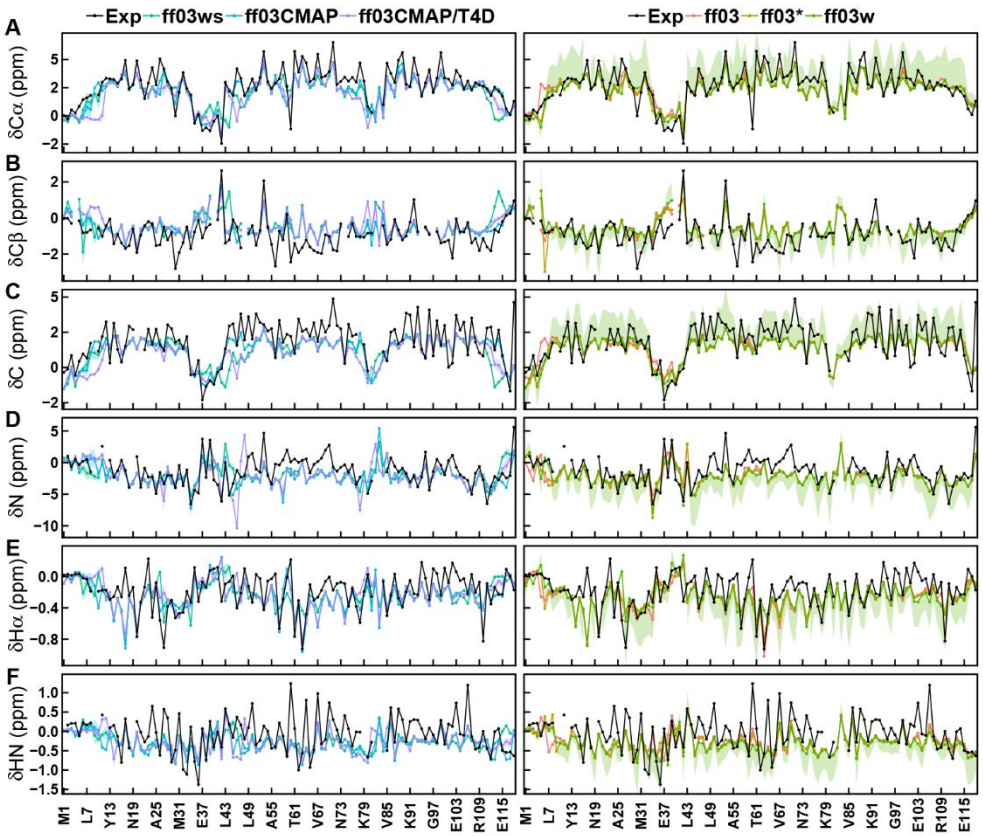

Figure S13. Secondary chemical shifts of simulation and experimental data for SPR17. Simulated and experimental secondary chemical shifts for (A) Cα, (B) Cβ, (C) C, (D) N, (E) Hα and (F) HN.

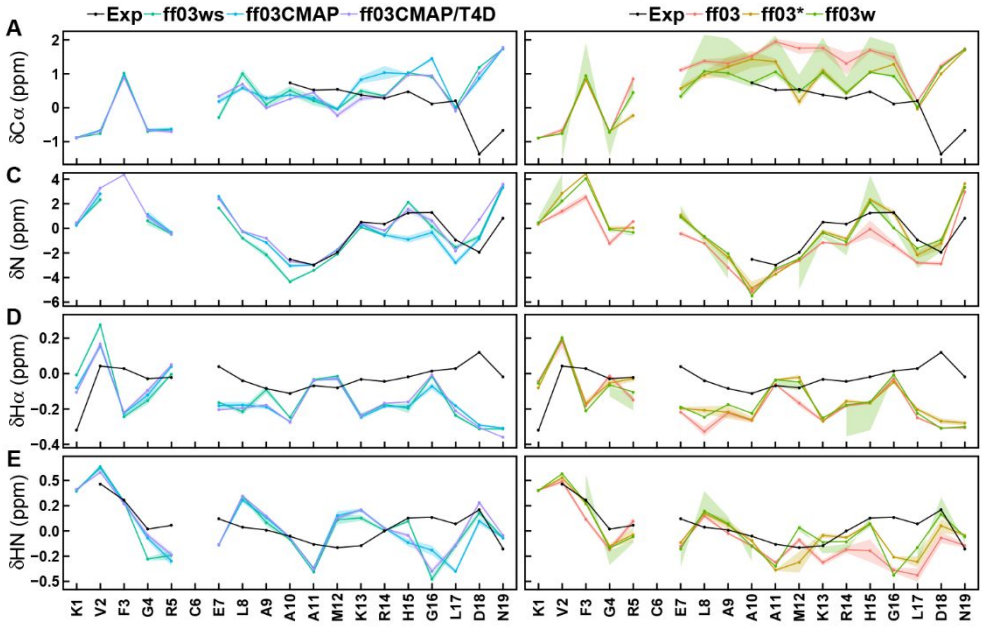

Figure S14. Secondary chemical shifts of simulation and experimental data for HEWL19. Simulated and experimental secondary chemical shifts for (A) Cα, (B) N, (C) Hα and (D) HN.

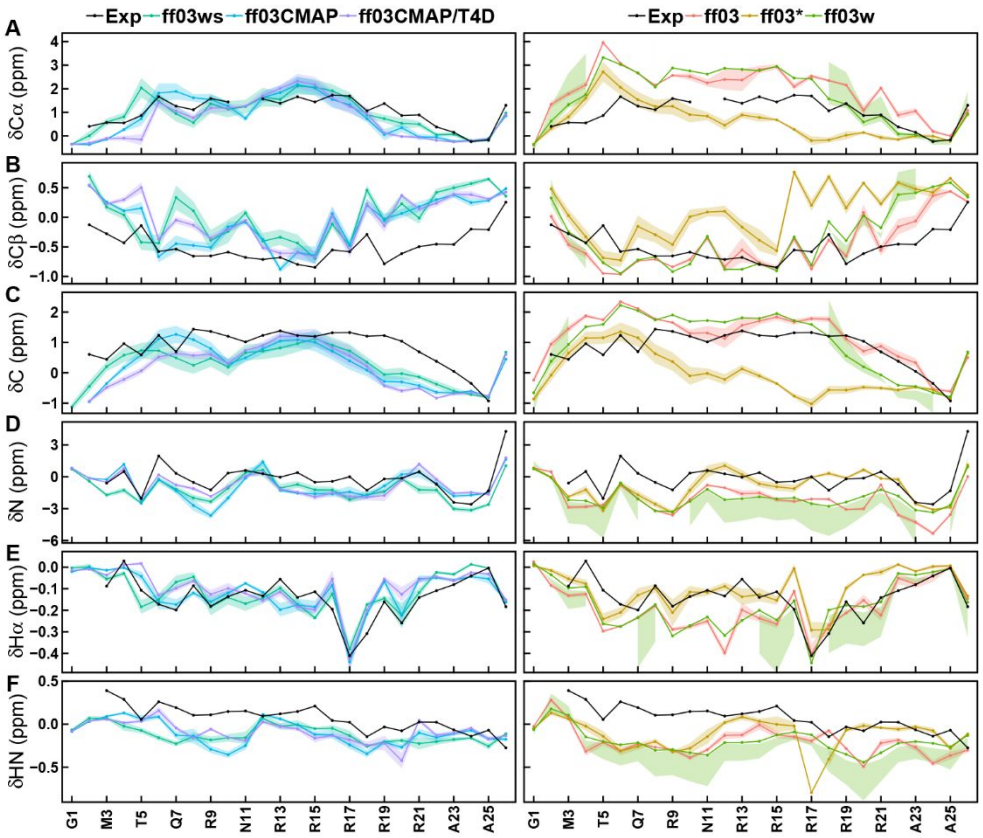

Figure S15. Secondary chemical shifts of simulation and experimental data for HIVRev. Simulated and experimental secondary chemical shifts for (A) Cα, (B) Cβ, (C) C, (D) N, (E) Hα and (F) HN.

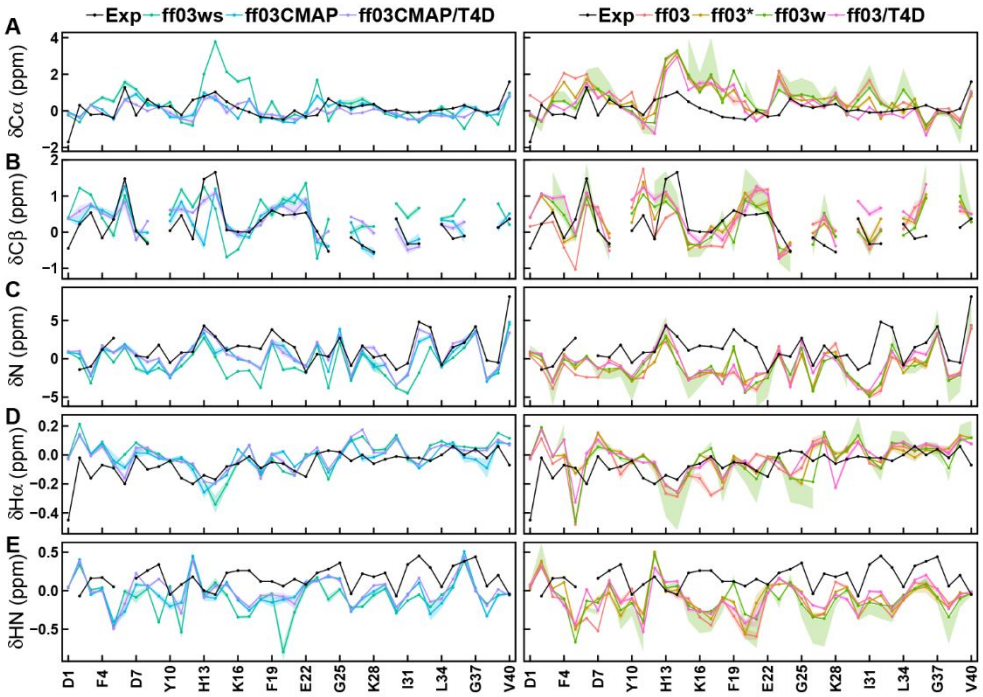

Figure S16. Secondary chemical shifts of simulation and experimental data for Aβ40. Simulated and experimental secondary chemical shifts for (A) Cα, (B) Cβ, (C) N, (D) Hα and (E) HN.

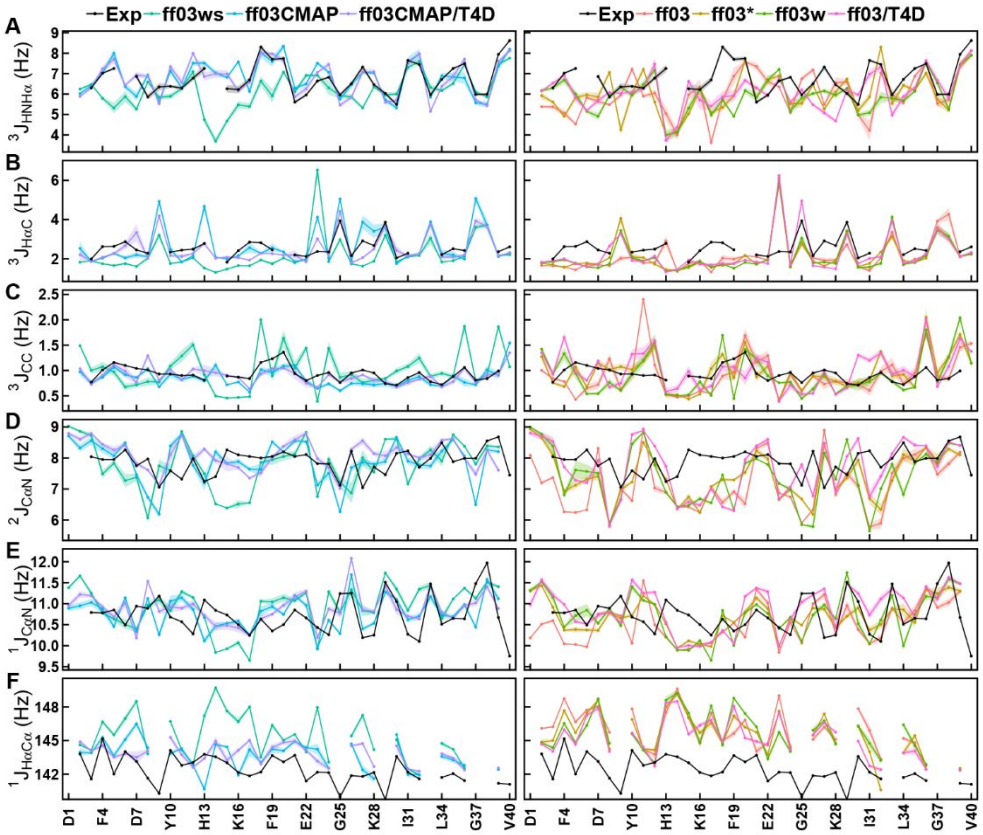

Figure S17. Scalar coupling constants of simulation and experimental data for Aβ40. Simulated and experimental scalar coupling constants for (A) $^{3}J_{HNH\alpha}$, (B) $^{3}J_{H\alpha C}$, (C) $^{3}J_{CC}$, (D) $^{2}J_{C\alpha N}$, (E) $^{1}J_{C\alpha N}$ and (F) $^{1}J_{H\alpha C\alpha}$.

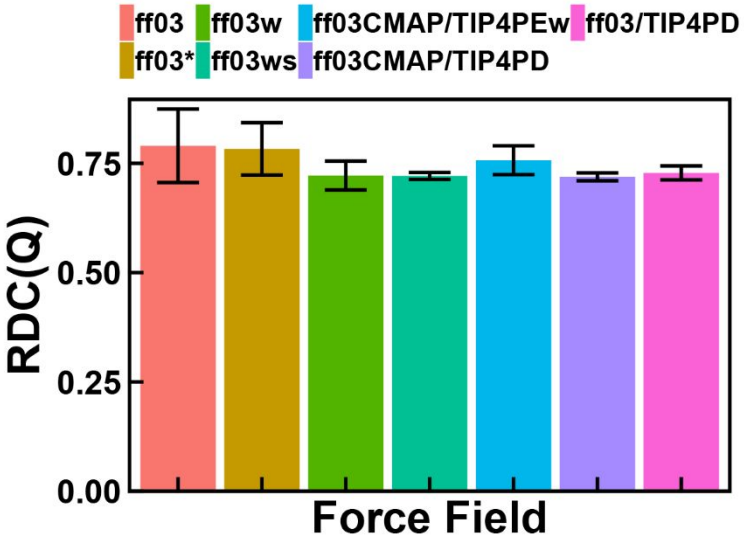

Figure S18. Backbone RDC of simulation of six ff03-series force fields for Aβ40. Error bar means the standard deviation of calculation.

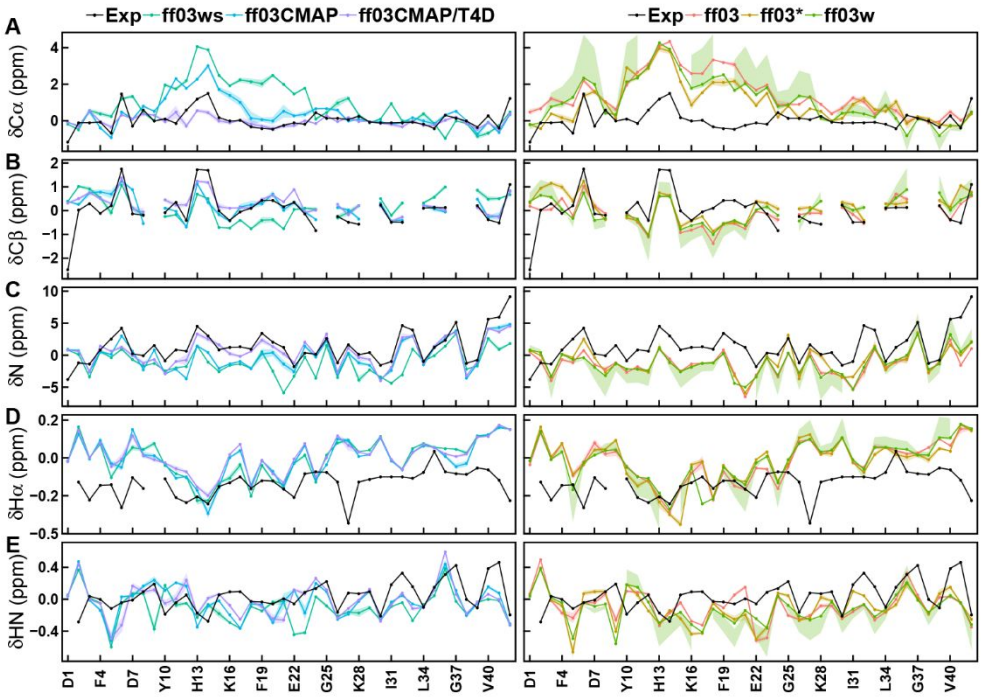

Figure S19. Secondary chemical shifts of simulation and experimental data for Aβ42. Simulated and experimental secondary chemical shifts for (A) Cα, (B) Cβ, (C) N, (D) Hα and (E) HN.

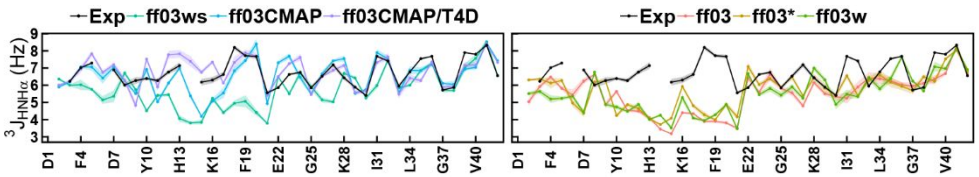

Figure S20. Scalar coupling constants of simulation and experimental data for Aβ42. Simulated and experimental scalar coupling constants for $^3J_{HNH\alpha}$.

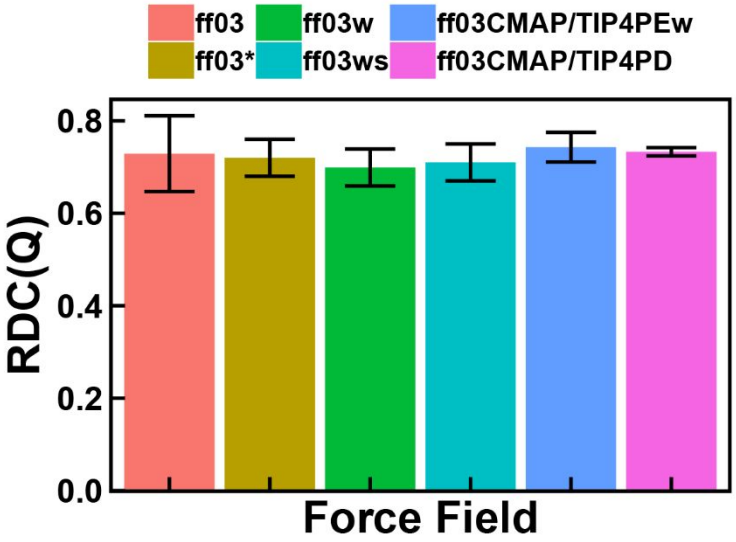

Figure S21. Backbone RDC of simulation of six ff03-series force fields for Aβ40. Error bar means the standard deviation of calculation.

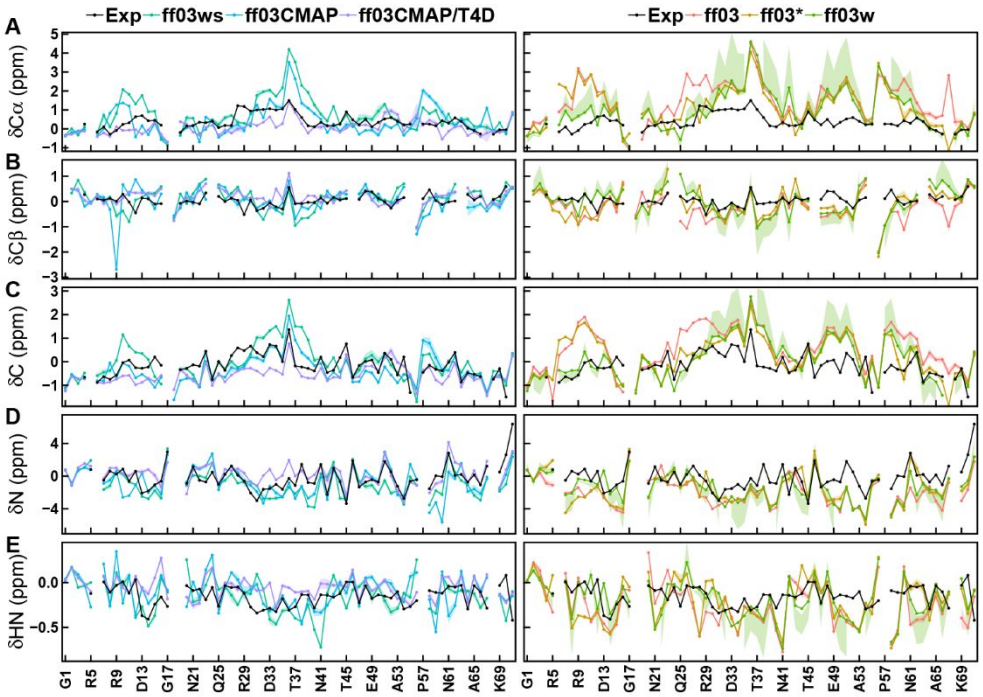

Figure S22. Secondary chemical shifts of simulation and experimental data for ACTR. Simulated and experimental secondary chemical shifts for (A) Cα, (B) Cβ, (C) C, (D) N and (E) HN.

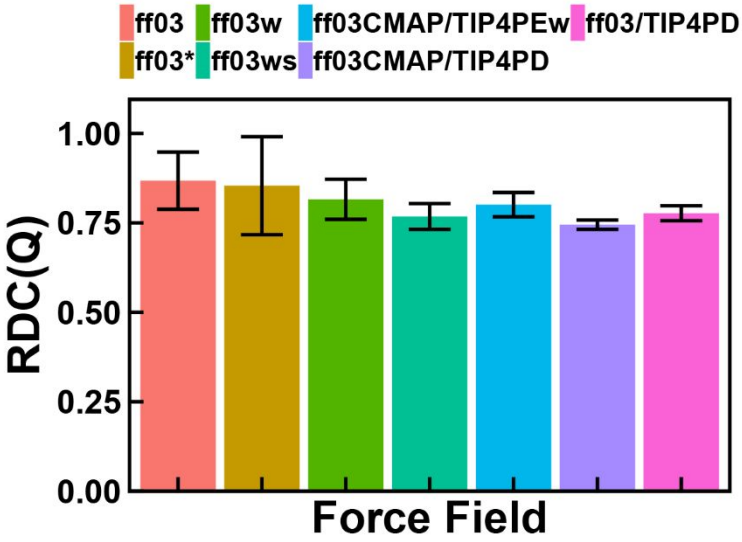

Figure S23. Backbone RDC of simulation of six ff03-series force fields for ACTR. Error bar means the standard deviation of calculation.

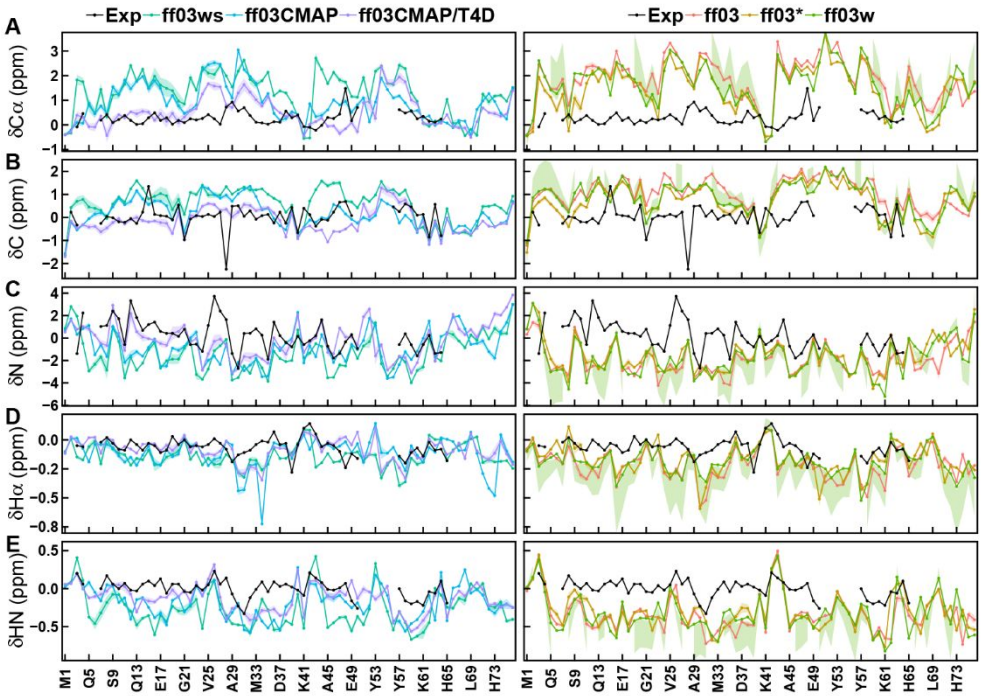

Figure S24. Secondary chemical shifts of simulation and experimental data for IA3. Simulated and experimental secondary chemical shifts for (A) Cα, (B) C, (C) N, (D) Hα and (E) HN.

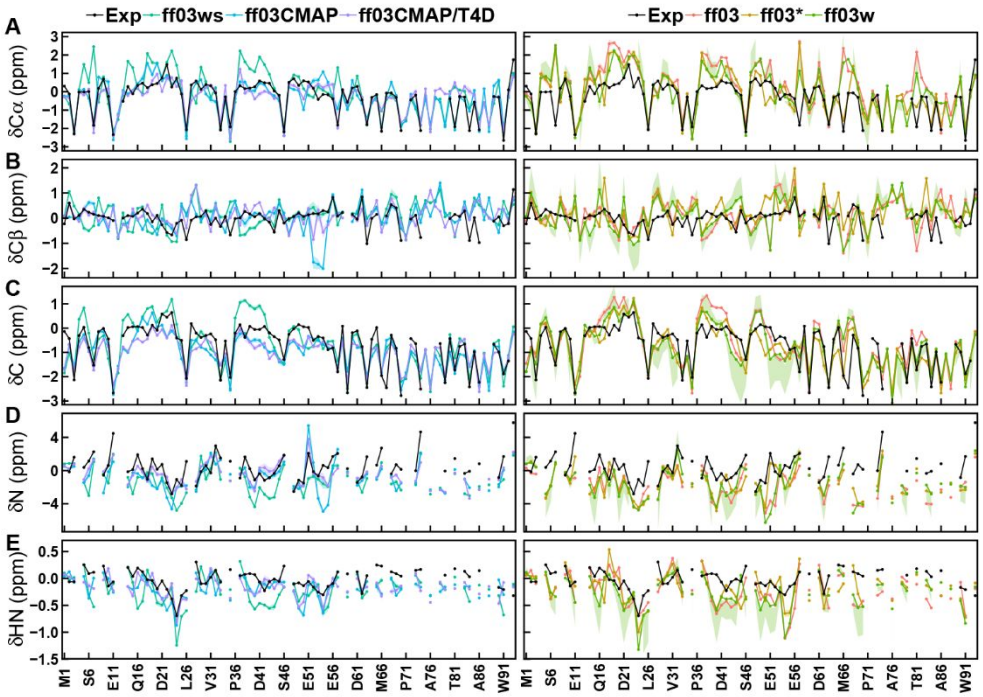

Figure S25. Secondary chemical shifts of simulation and experimental data for p53N. Simulated and experimental secondary chemical shifts for (A) Cα, (B) Cβ, (C) C, (D) N and (E) HN.

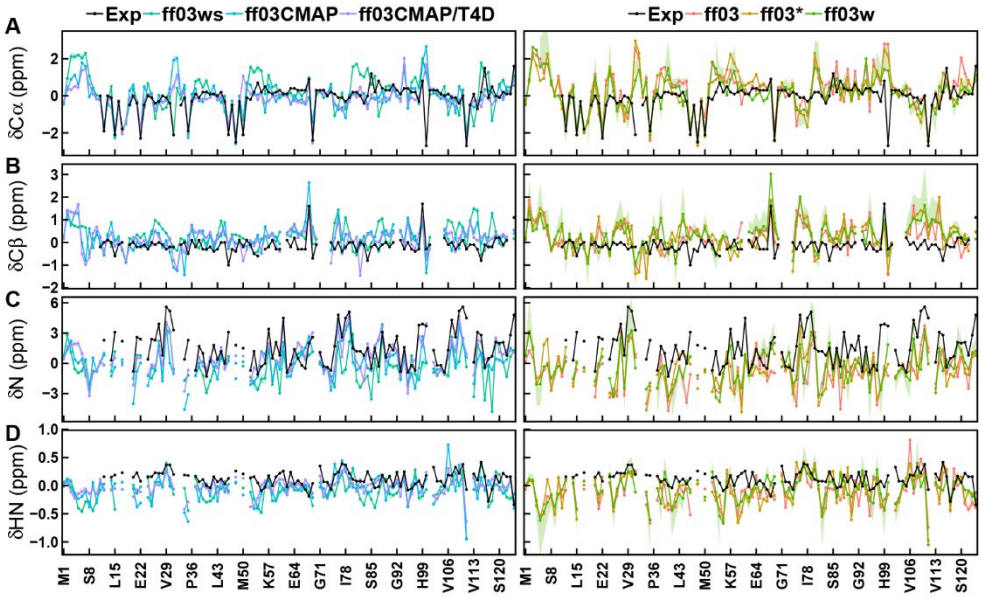

Figure S26. Secondary chemical shifts of simulation and experimental data for tauF4. Simulated and experimental secondary chemical shifts for (A) Cα, (B) Cβ, (C) N and (D) HN.

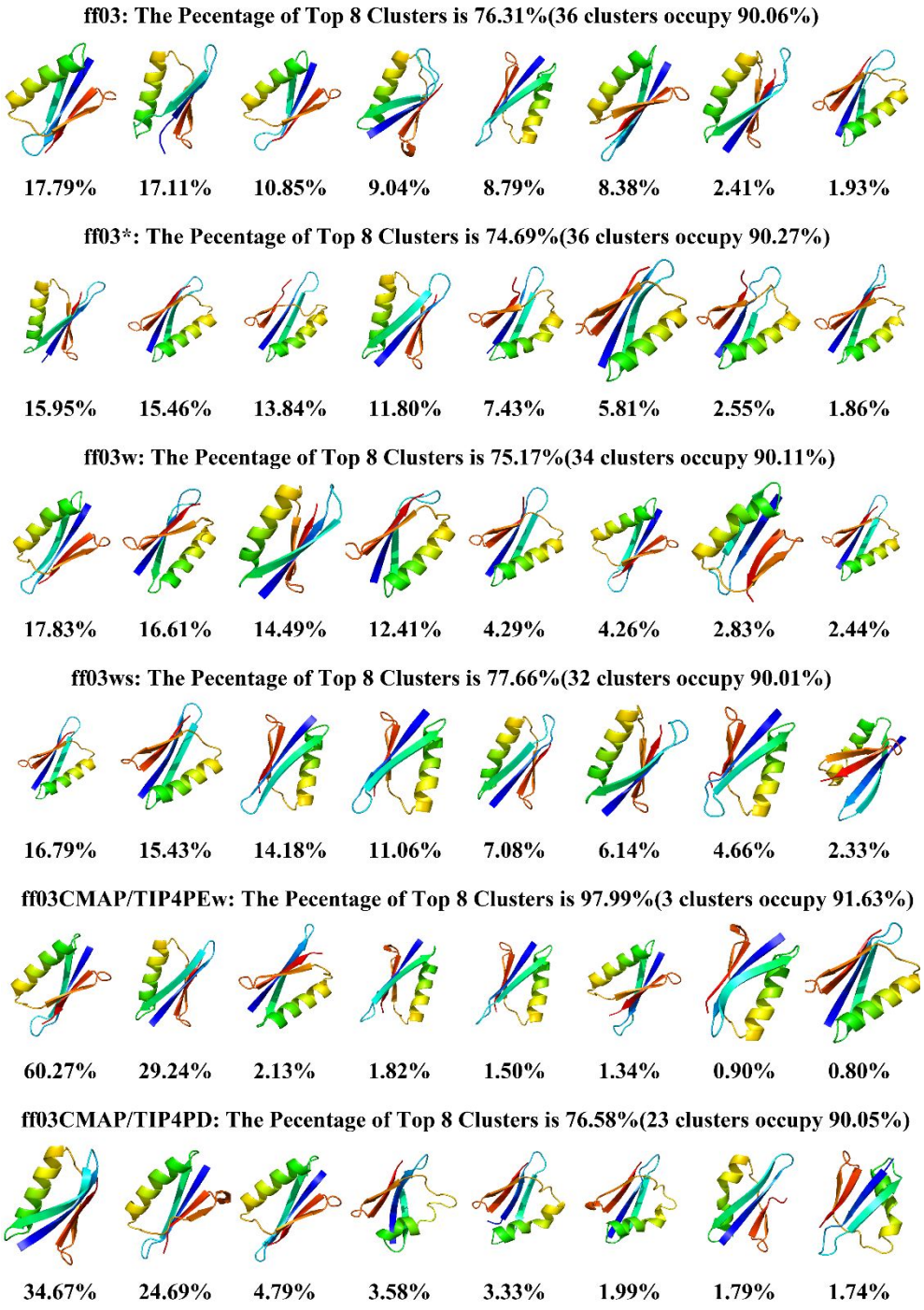

Figure S27. Conformation clustering of simulation for GB3. For each force field, we showed delegate conformations of top 8 clusters at most. And we showed the information of population of displayed conformation and numbers of clusters occupy just more than 90% for each force field.

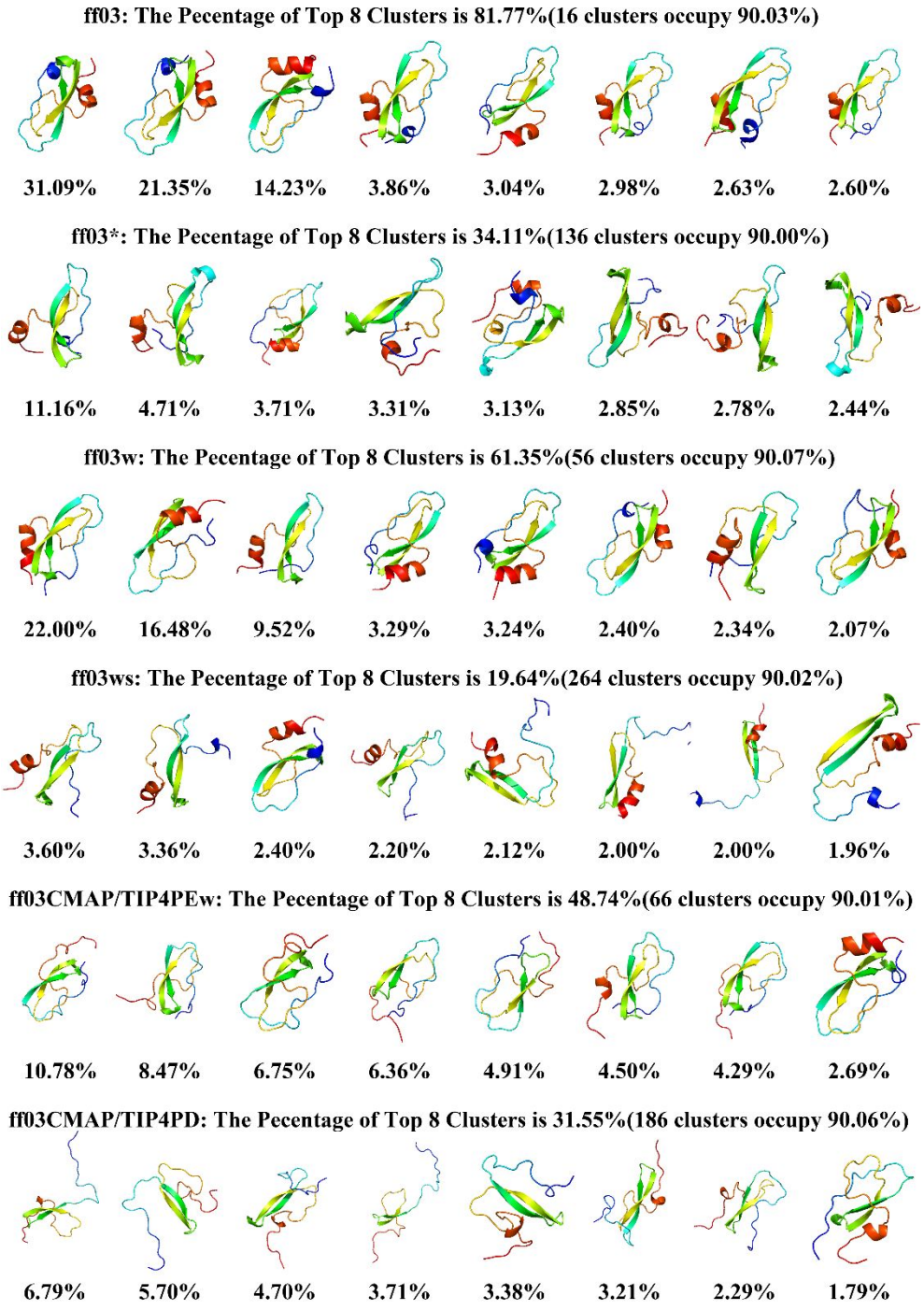

Figure S28. Conformation clustering of simulation for BPTI.

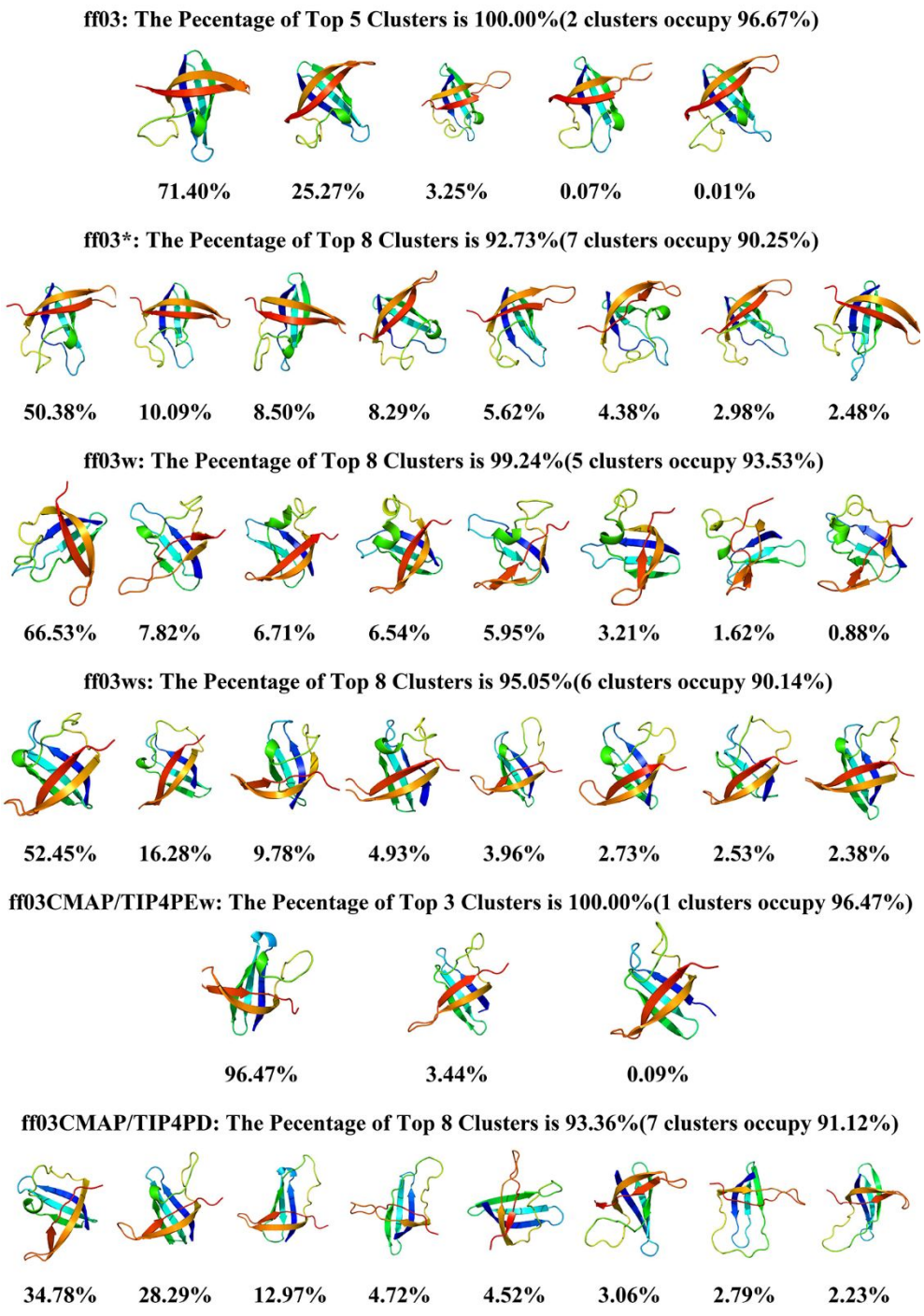

Figure S29. Conformation clustering of simulation for CspTm.

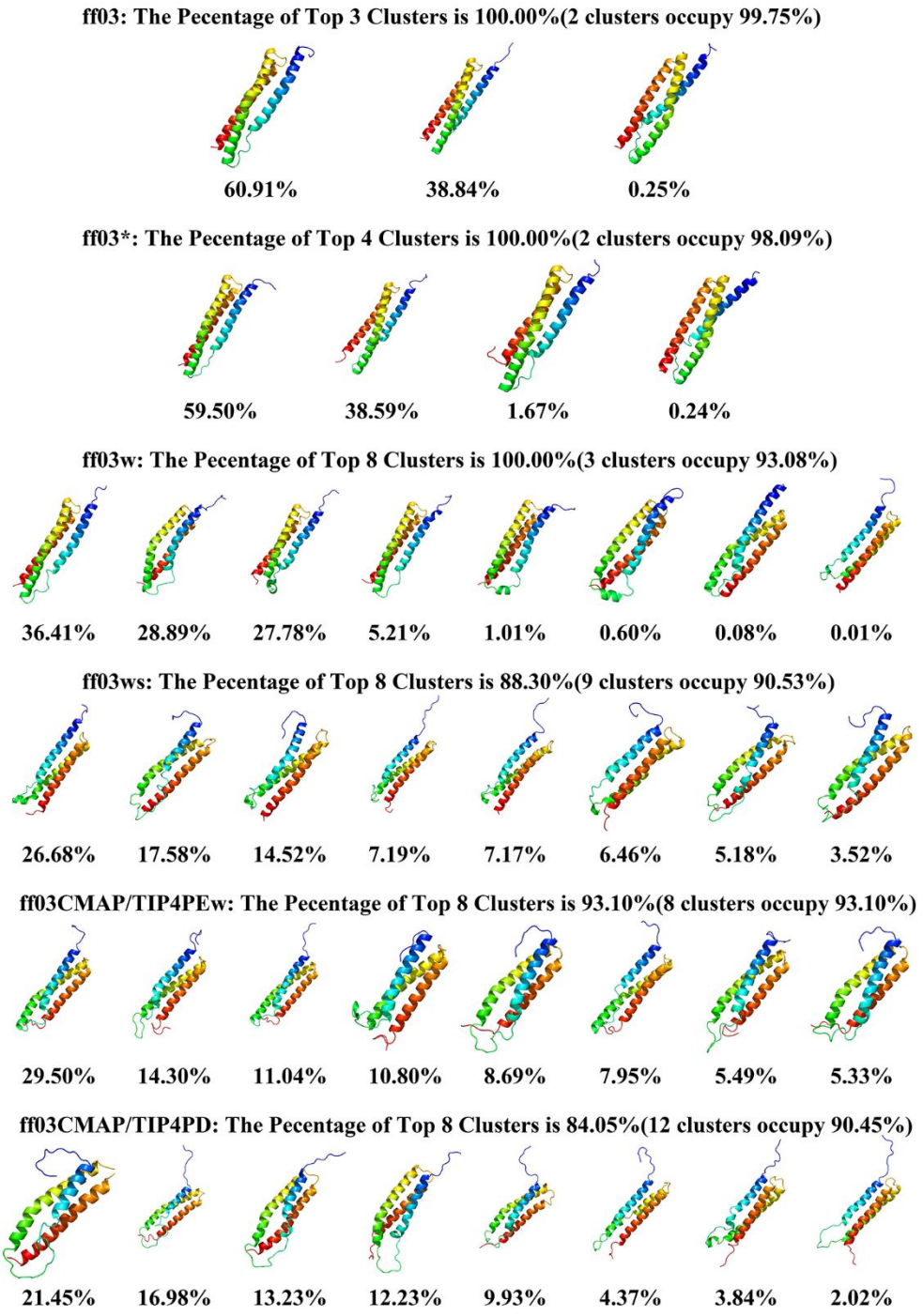

Figure S30. Conformation clustering of simulation for SPR17.

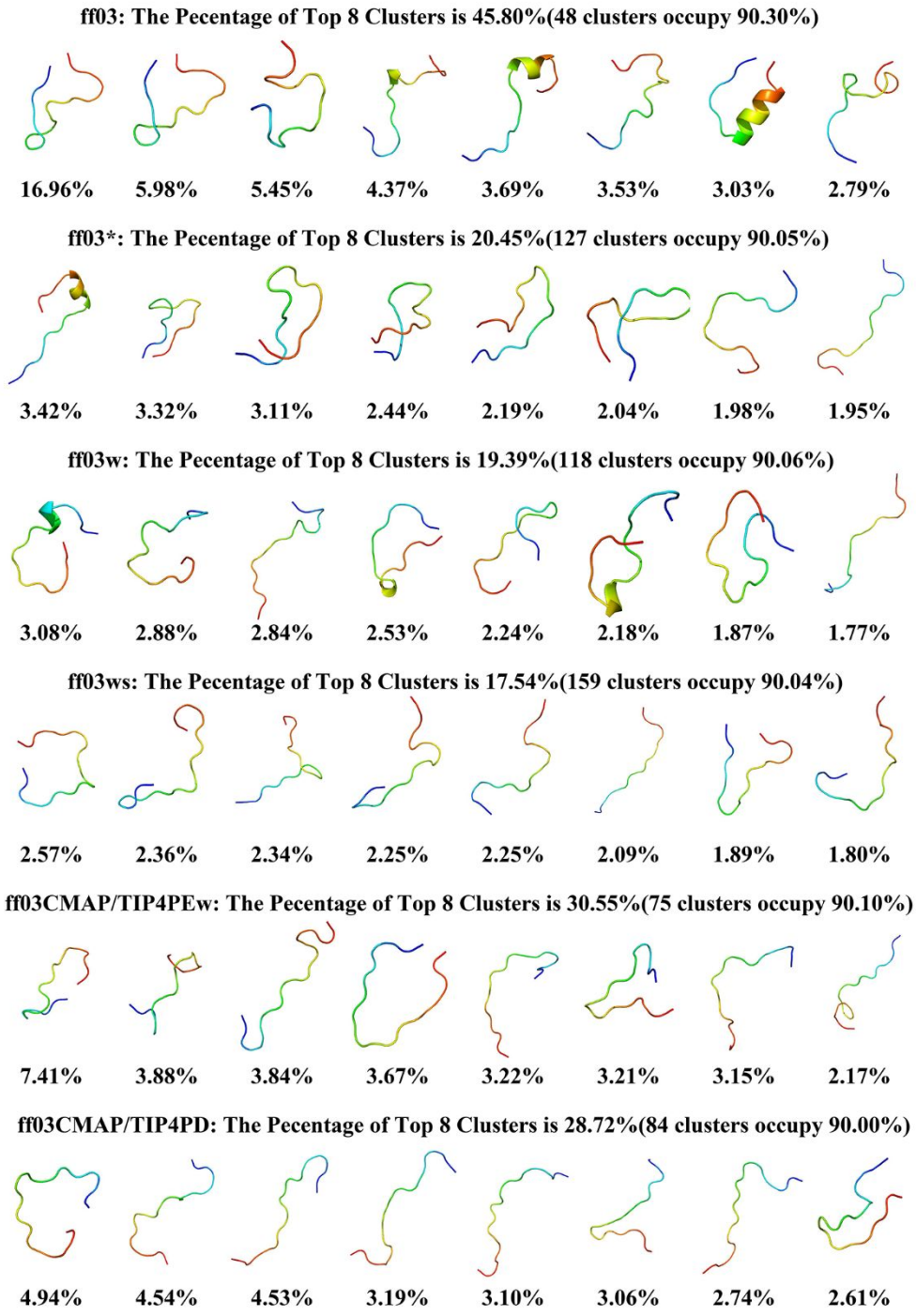

Figure S31. Conformation clustering of simulation for HEWL19.

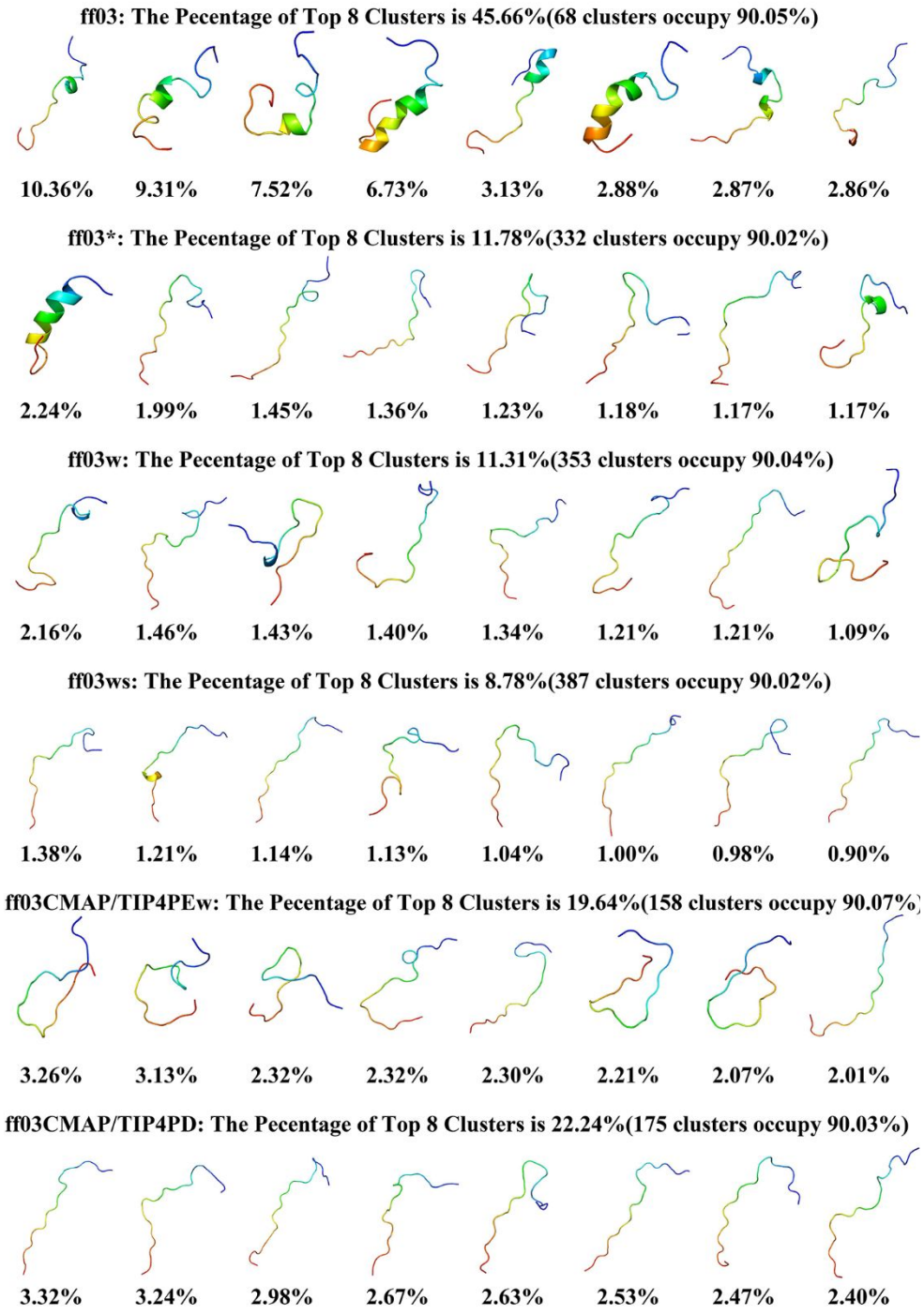

Figure S32. Conformation clustering of simulation for RS.

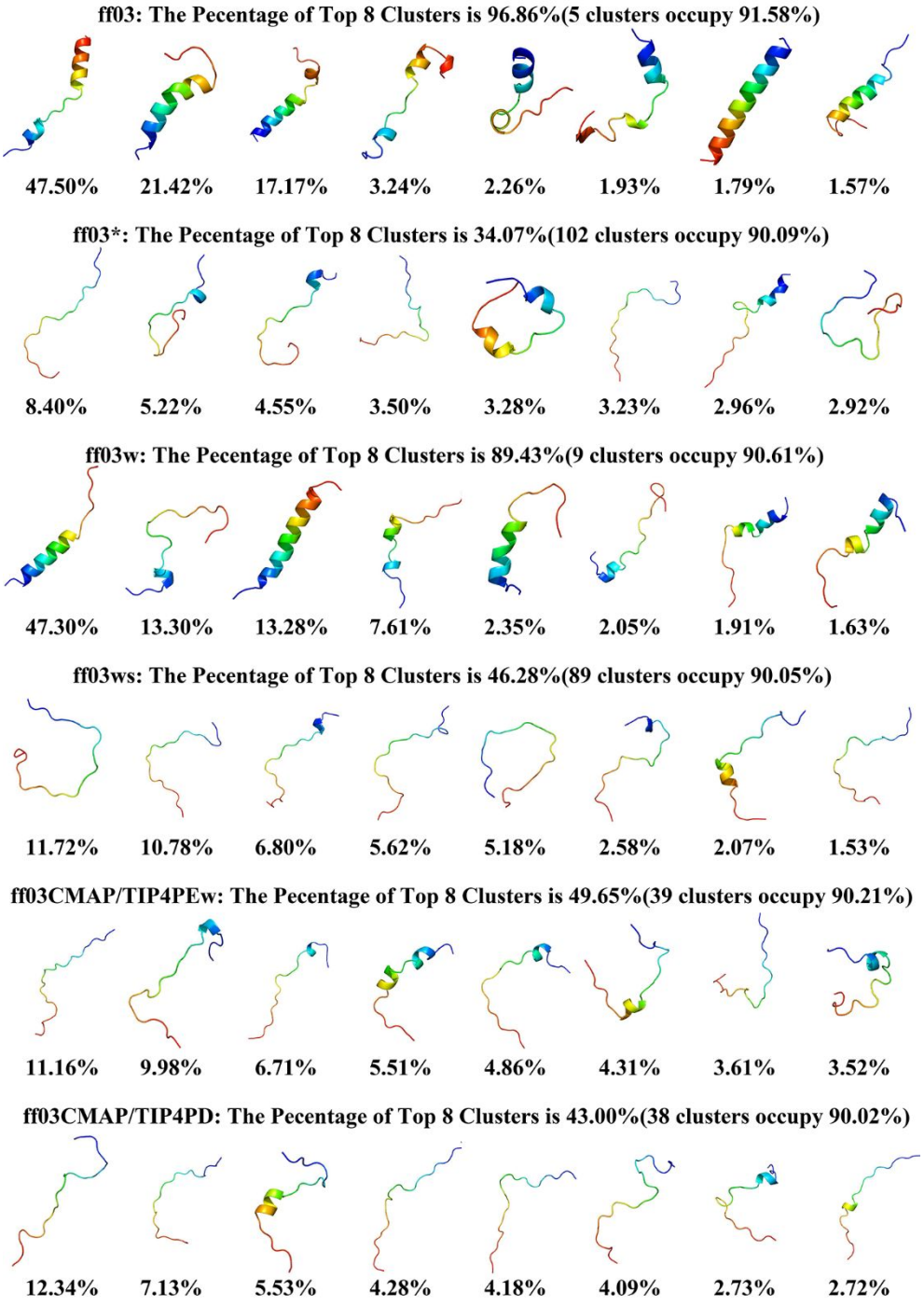

Figure S33. Conformation clustering of simulation for HIVRev.

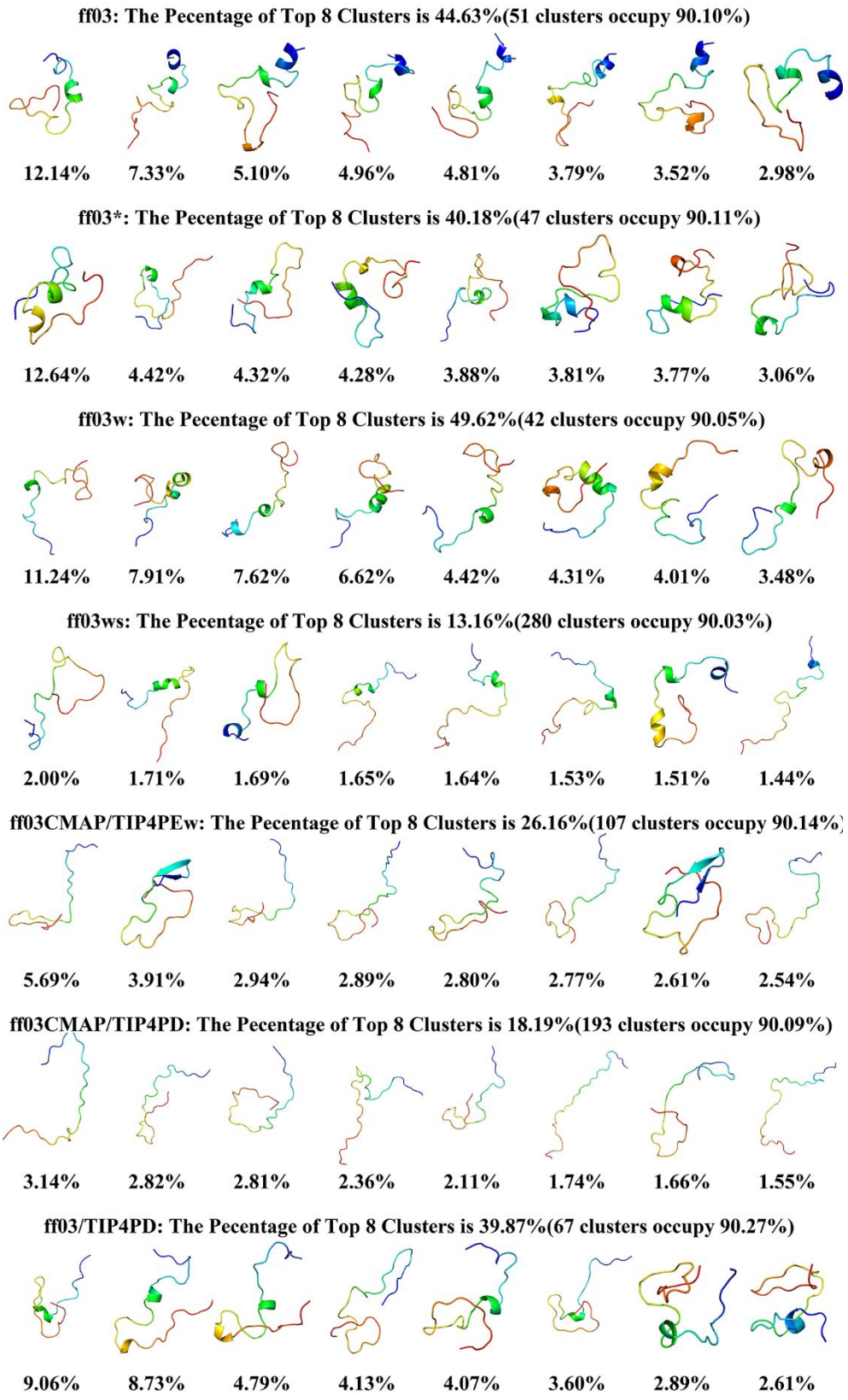

Figure S34. Conformation clustering of simulation for Aβ40.

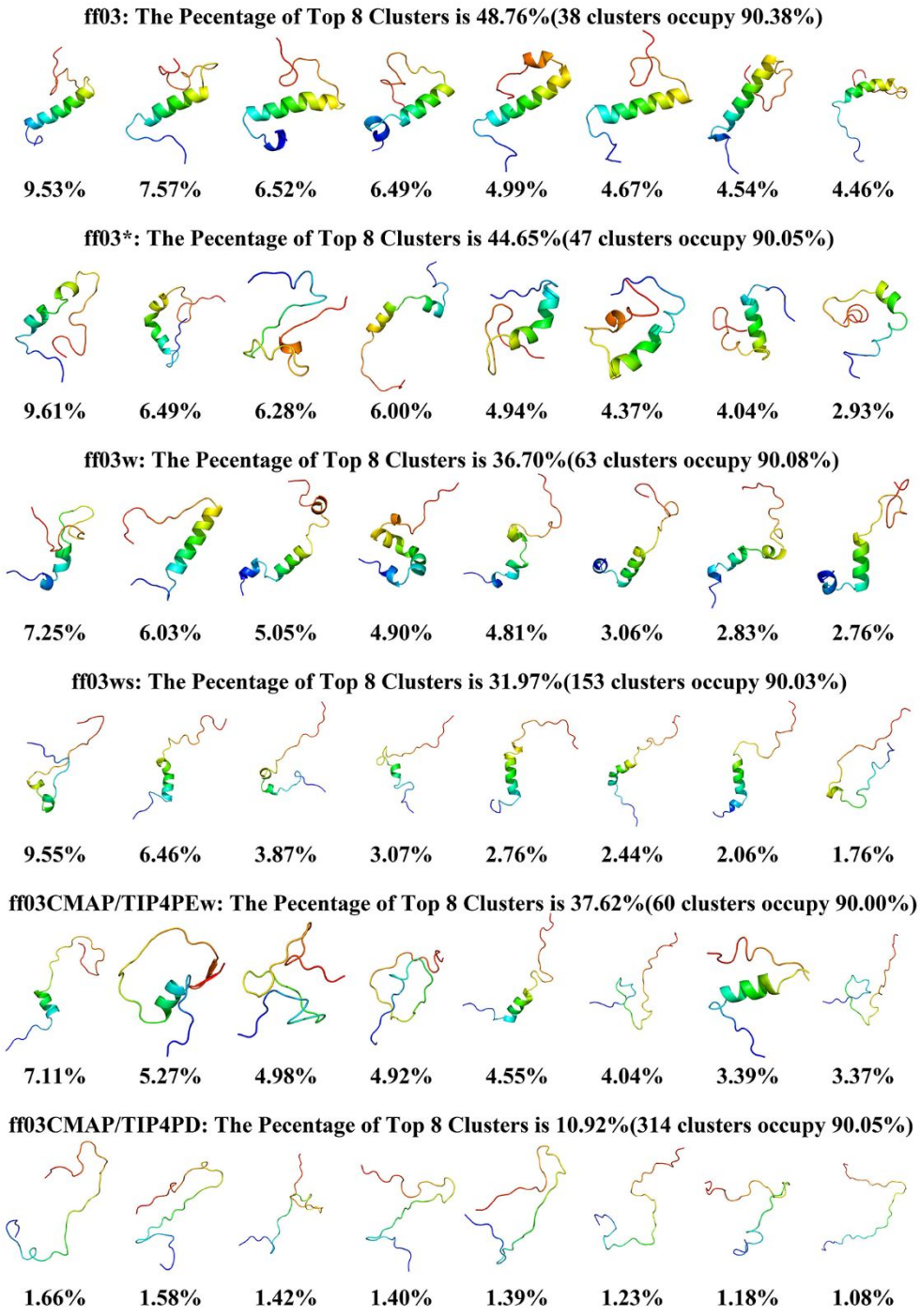

Figure S35. Conformation clustering of simulation for Aβ42.

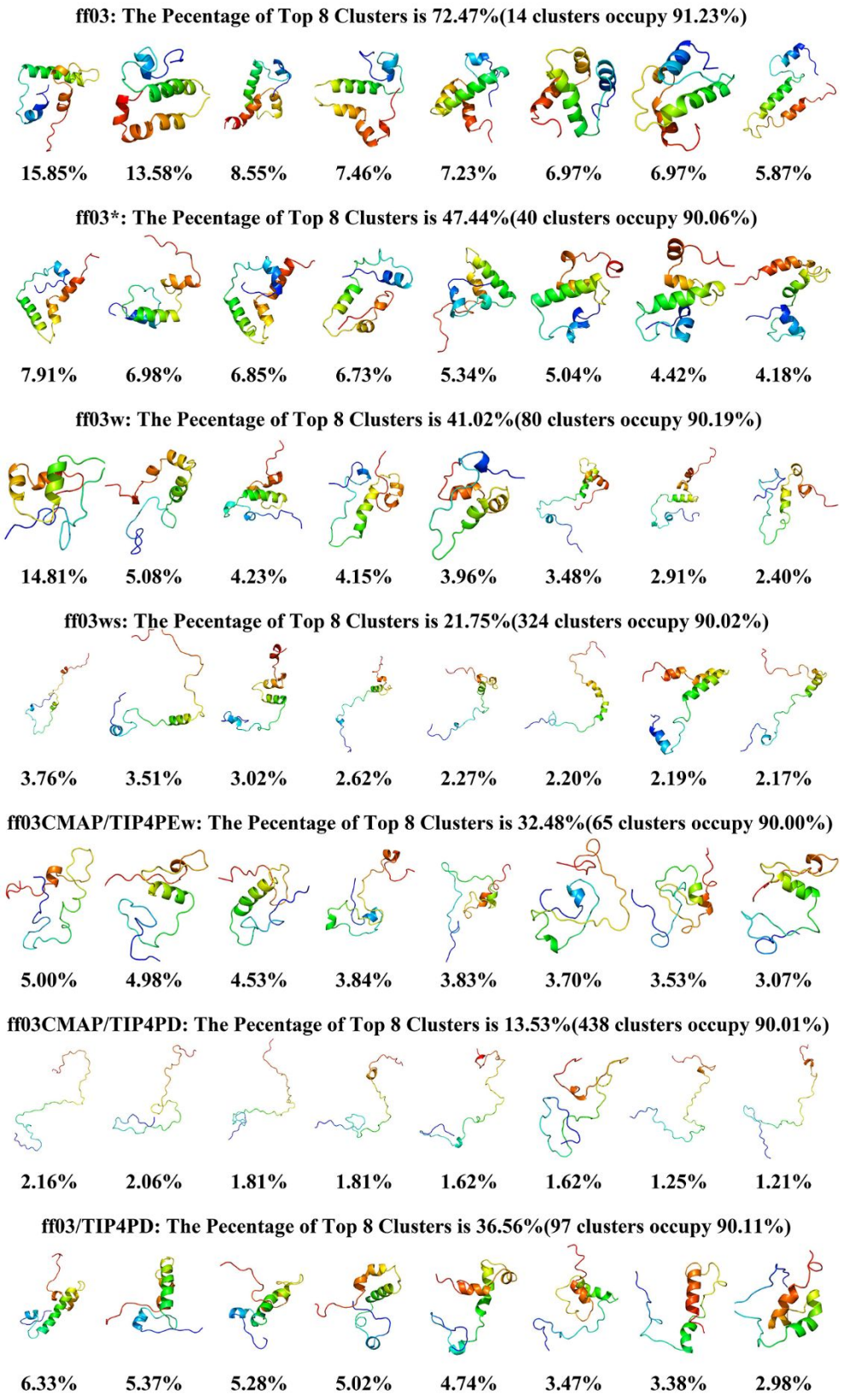

Figure S36. Conformation clustering of simulation for ACTR.

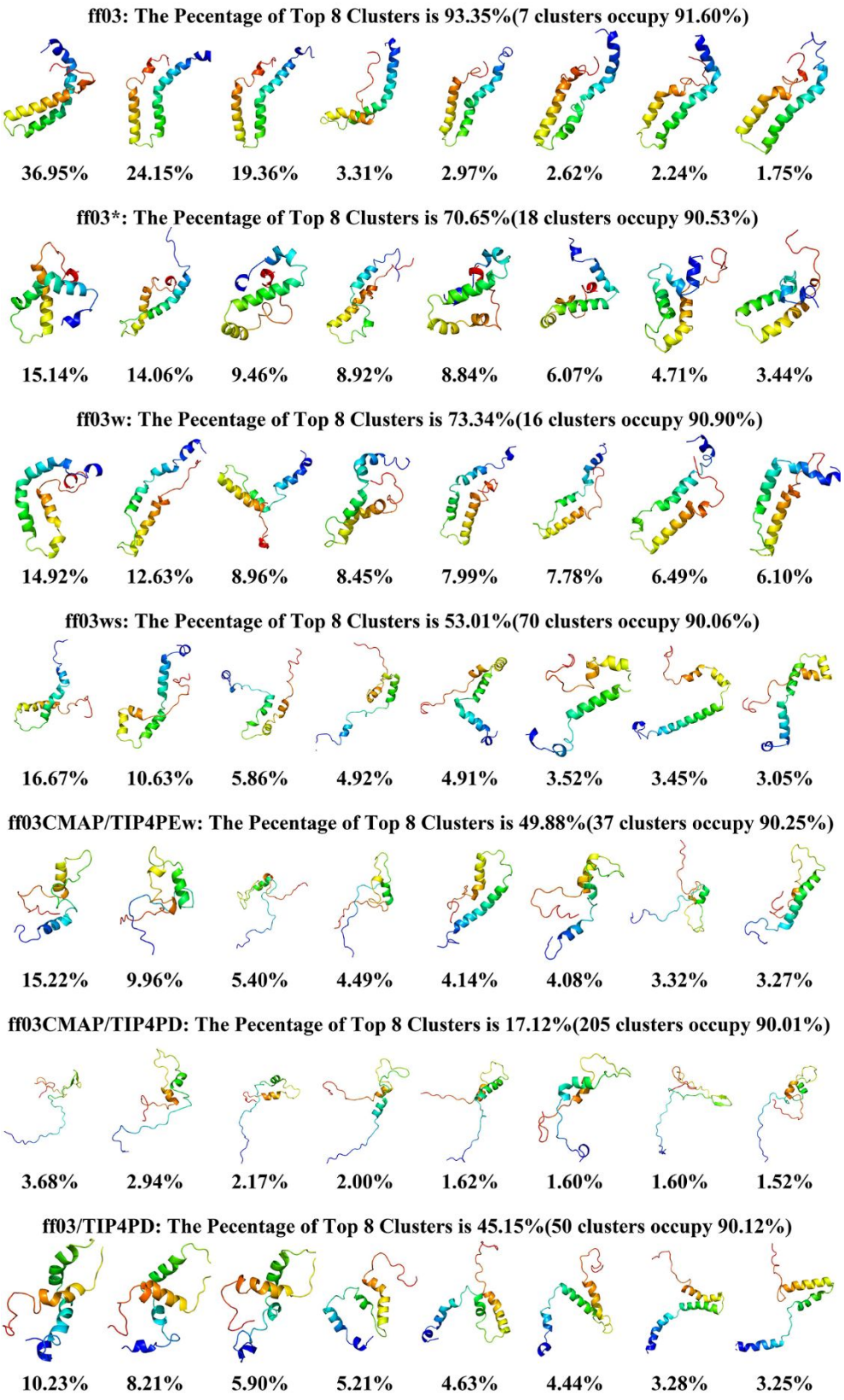

Figure S37. Conformation clustering of simulation for IA3.

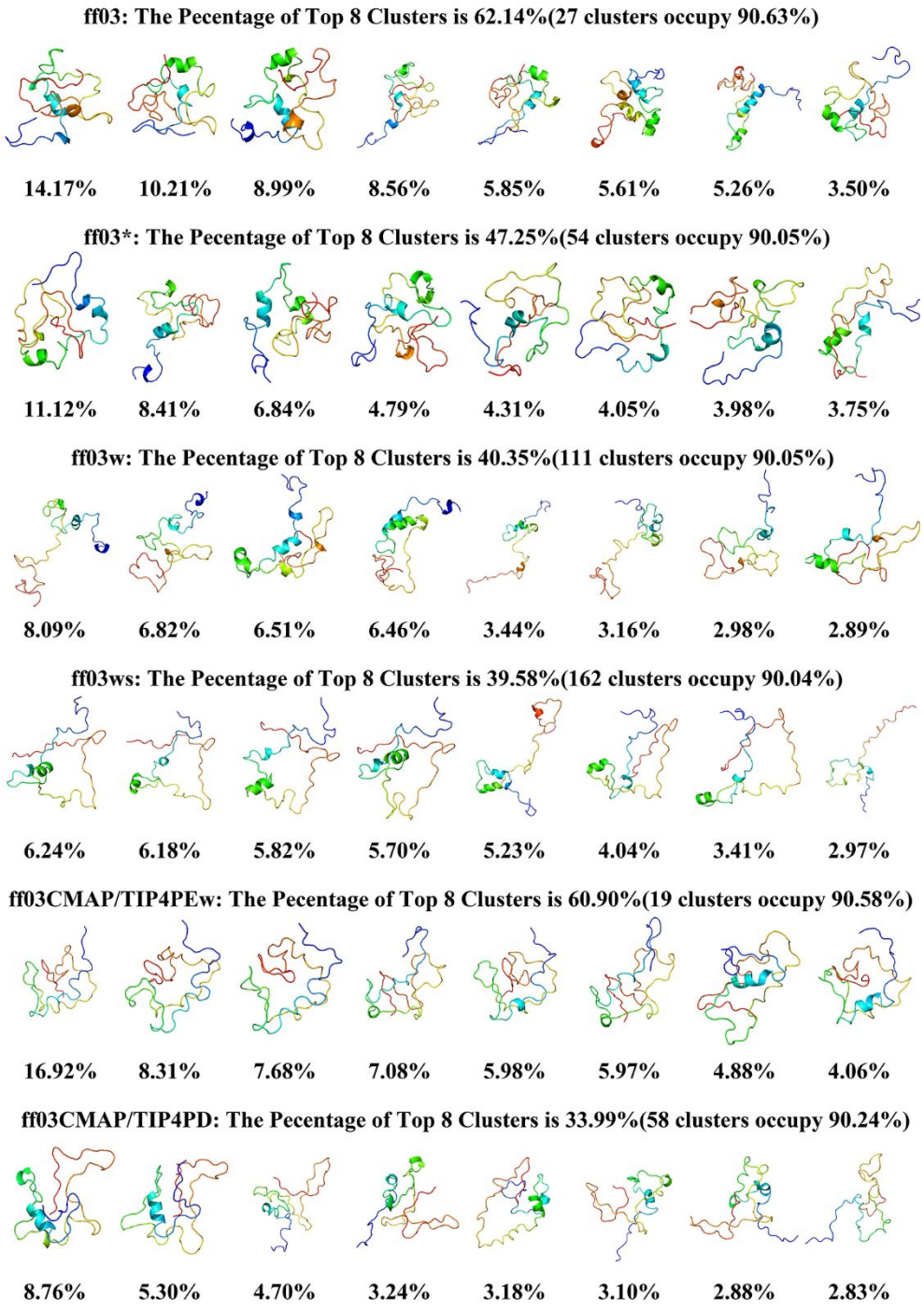

Figure S38. Conformation clustering of simulation for p53N.

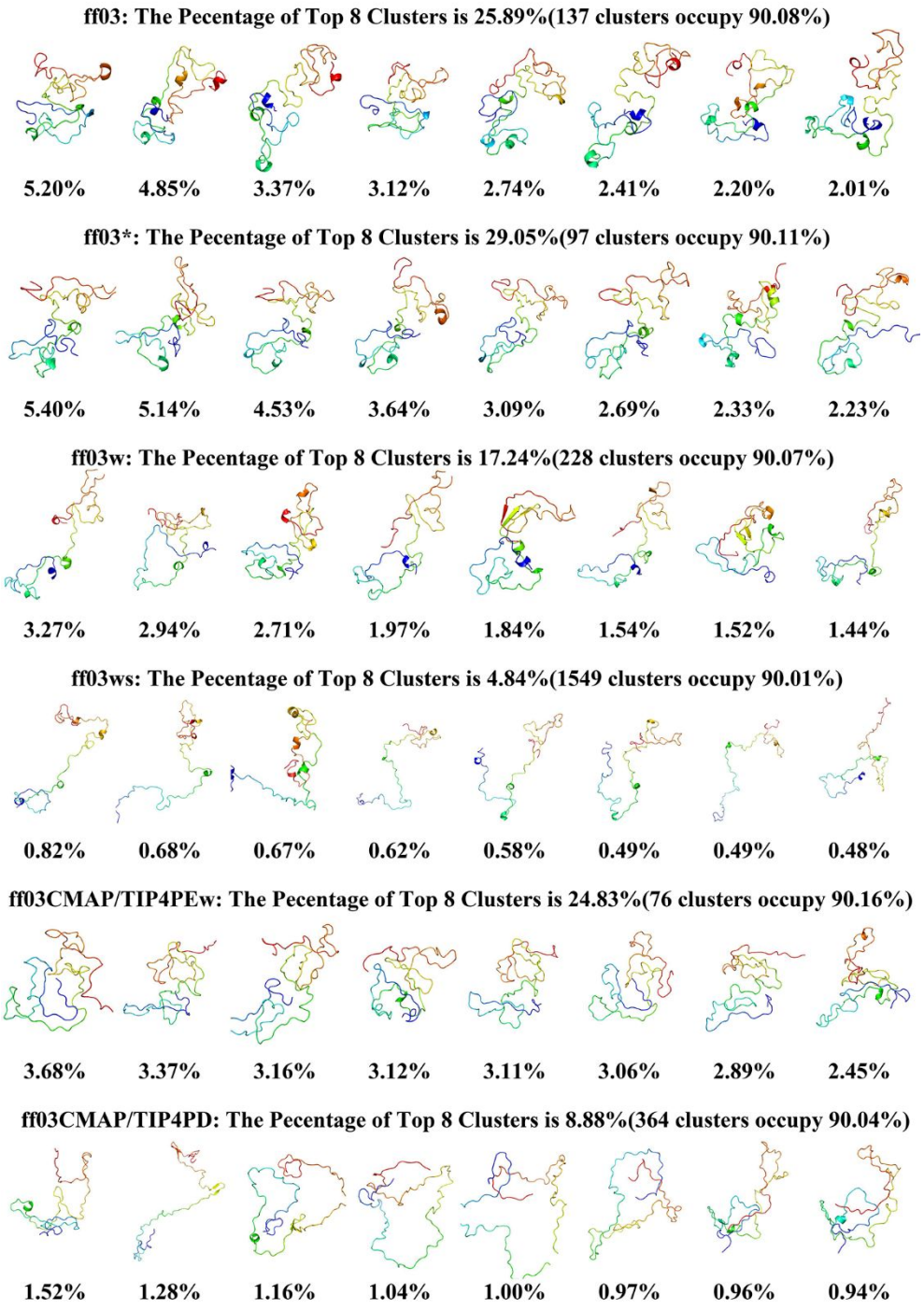

Figure S39. Conformation clustering of simulation for tauF4.

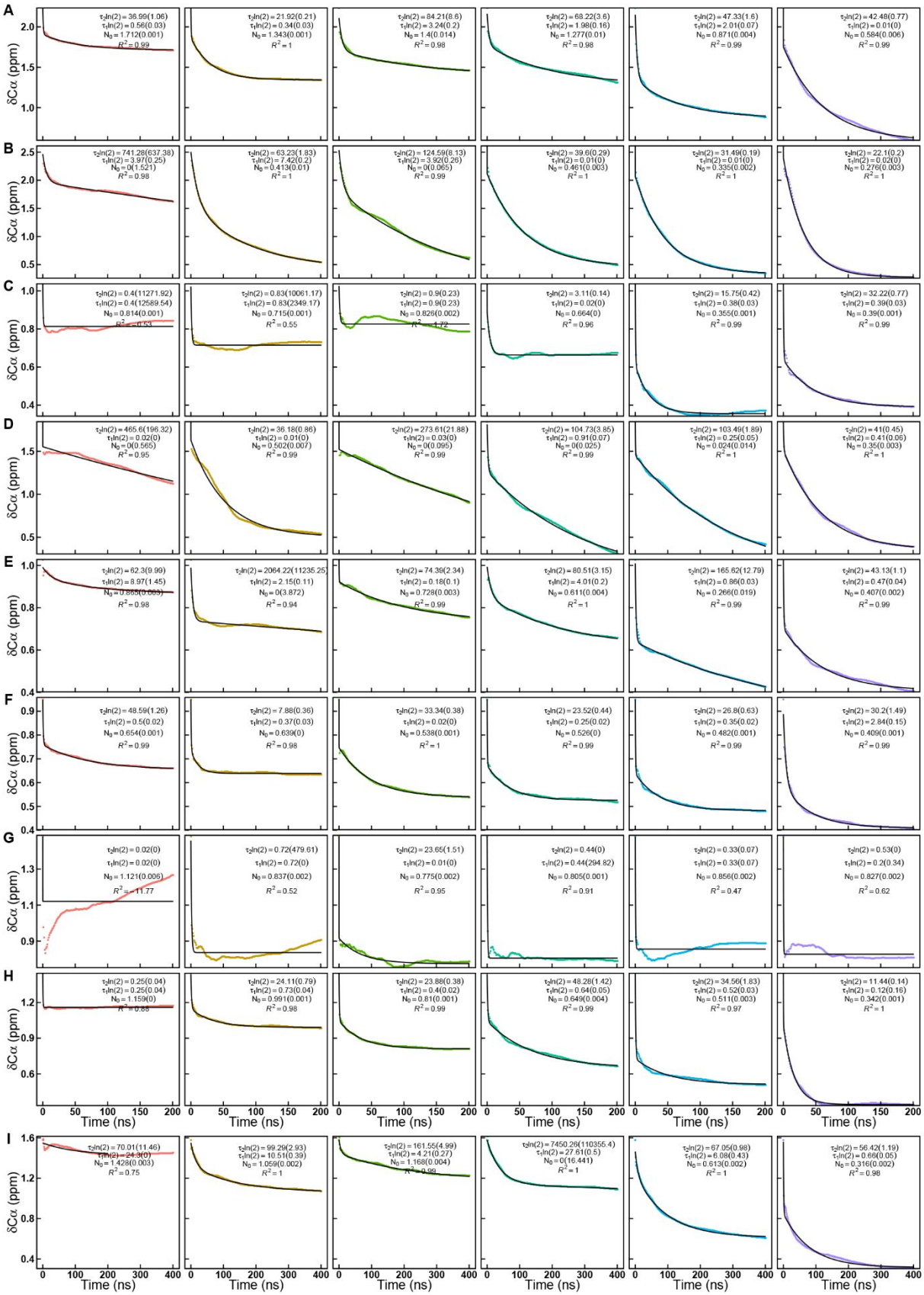

Figure S40. Biphasic exponential decay model fitting for disordered proteins. (A) IA3, (B) RS, (C) Aβ40, (D) HIVRev, (E) p53N, (F) tauF4, (G) HEWL19 (H) ACTR for 200ns MD simulation and (I) Aβ42 for 400ns MD simulation. Black solid line means the fit curve and colored dot means the simulated values for different force fields. τ_1 and τ_2 are in nanosecond, N_0 is in ppm, and R^2 is unitless.

Reference:

[1].Best, R. B.; Hummer, G., Optimized molecular dynamics force fields applied to the helix-coil transition of polypeptides. *The journal of physical chemistry. B* **2009,** *113* (26), 9004-15.

[2].Graf, J.; Nguyen, P. H.; Stock, G.; Schwalbe, H., Structure and dynamics of the homologous series of alanine peptides: a joint molecular dynamics/NMR study. *Journal of the American Chemical Society* **2007,** *129* (5), 1179-89.

[3].Vogeli, B.; Kazemi, S.; Guntert, P.; Riek, R., Spatial elucidation of motion in proteins by ensemble-based structure calculation using exact NOEs. *Nat Struct Mol Biol* **2012,** *19* (10), 1053-7.

[4].Vogeli, B.; Ying, J.; Grishaev, A.; Bax, A., Limits on variations in protein backbone dynamics from precise measurements of scalar couplings. *Journal of the American Chemical Society* **2007,** *129* (30), 9377-85.

[5].Yao, L.; Grishaev, A.; Cornilescu, G.; Bax, A., Site-specific backbone amide (15)N chemical shift anisotropy tensors in a small protein from liquid crystal and cross-correlated relaxation measurements. *Journal of the American Chemical Society* **2010,** *132* (12), 4295-309.

[6].Biamonti, C., Structural and dynamic investigations of macromolecular recognition processes by nuclear magnetic resonance spectroscopy. **1997**.

[7].Balasubramanian, S.; Nirmala, R.; Beveridge, D. L.; Bolton, P. H., Comparison of the 13C relaxation times and proton scalar couplings of BPTI with values predicted by molecular dynamics. *J Magn Reson B* **1994,** *104* (3), 240-9.

[8].Kremer, W.; Schuler, B.; Harrieder, S.; Geyer, M.; Gronwald, W.; Welker, C.; Jaenicke, R.; Kalbitzer, H. R., Solution NMR structure of the cold-shock protein from the hyperthermophilic bacterium Thermotoga maritima. *Eur J Biochem* **2001,** *268* (9), 2527-39.

[9].Cornilescu, G.; Marquardt, J. L.; Ottiger, M.; Bax, A., Validation of protein structure from anisotropic carbonyl chemical shifts in a dilute liquid crystalline phase. *Journal of the American Chemical Society* **1998,** *120* (27), 6836-6837.

[10].Wang, A. C.; Bax, A., Determination of the backbone dihedral angles φ in human ubiquitin from reparametrized empirical Karplus equations. *Journal of the American Chemical Society* **1996,** *118* (10), 2483-2494.

[11].Schmidt, J. M.; Hua, Y.; Lohr, F., Correlation of (2)J couplings with protein secondary structure. *Proteins* **2010,** *78* (6), 1544-62.

[12].Schmidt, J. M.; Howard, M. J.; Maestre-Martinez, M.; Perez, C. S.; Lohr, F., Variation in protein C(alpha)-related one-bond J couplings. *Magn Reson Chem* **2009,** *47* (1), 16-30.

[13].Chou, J. J.; Case, D. A.; Bax, A., Insights into the mobility of methyl-bearing side chains in proteins from 3 J CC and 3 J CN couplings. *Journal of the American Chemical Society* **2003,** *125* (29), 8959-8966.

[14].Ottiger, M.; Bax, A., Determination of Relative N− HN, N− C ‘, Cα− C ‘, and Cα− Hα Effective Bond Lengths in a Protein by NMR in a Dilute Liquid Crystalline Phase. *Journal of the American Chemical Society* **1998,** *120* (47), 12334-12341.

[15].Hus, J. C.; Peti, W.; Griesinger, C.; Bruschweiler, R., Self-consistency analysis of dipolar couplings in multiple alignments of ubiquitin. *Journal of the American Chemical Society* **2003,** *125* (19), 5596-7.

[16].Tjandra, N.; Feller, S. E.; Pastor, R. W.; Bax, A., Rotational diffusion anisotropy of human ubiquitin from 15N NMR relaxation. *Journal of the American Chemical Society* **1995,** *117* (50), 12562-12566.

[17].Lee, A. L.; Flynn, P. F.; Wand, A. J., Comparison of 2H and 13C NMR relaxation techniques for the study of protein methyl group dynamics in solution. *Journal of the American Chemical Society* **1999,** *121* (12), 2891-2902.

[18].Brenner, A. K.; Kieffer, B.; Trave, G.; Froystein, N. A.; Raae, A. J., Thermal stability of chicken brain alpha-spectrin repeat 17: a spectroscopic study. *J Biomol NMR* **2012,** *53* (2), 71-83.

[19].Xiang, S.; Gapsys, V.; Kim, H. Y.; Bessonov, S.; Hsiao, H. H.; Mohlmann, S.; Klaukien, V.; Ficner, R.; Becker, S.; Urlaub, H.; Luhrmann, R.; de Groot, B.; Zweckstetter, M., Phosphorylation drives a dynamic switch in serine/arginine-rich proteins. *Structure* **2013,** *21* (12), 2162-74.

[20].Rauscher, S.; Gapsys, V.; Gajda, M. J.; Zweckstetter, M.; de Groot, B. L.; Grubmuller, H., Structural Ensembles of Intrinsically Disordered Proteins Depend Strongly on Force Field: A Comparison to Experiment. *Journal of chemical theory and computation* **2015,** *11* (11), 5513-24.

[21].Casu, F.; Duggan, B. M.; Hennig, M., The arginine-rich RNA-binding motif of HIV-1 Rev is intrinsically disordered and folds upon

RRE binding. *Biophys J* **2013,** *105* (4), 1004-17.
[22].Yamaguchi, T.; Matsuzaki, K.; Hoshino, M., Transient formation of intermediate conformational states of amyloid-beta peptide revealed by heteronuclear magnetic resonance spectroscopy. *FEBS Lett* **2011,** *585* (7), 1097-102.
[23].Roche, J.; Shen, Y.; Lee, J. H.; Ying, J.; Bax, A., Monomeric Abeta(1-40) and Abeta(1-42) Peptides in Solution Adopt Very Similar Ramachandran Map Distributions That Closely Resemble Random Coil. *Biochemistry* **2016,** *55* (5), 762-75.
[24].Yan, Y.; McCallum, S. A.; Wang, C., M35 oxidation induces Abeta40-like structural and dynamical changes in Abeta42. *Journal of the American Chemical Society* **2008,** *130* (16), 5394-5.
[25].Granata, D.; Baftizadeh, F.; Habchi, J.; Galvagnion, C.; De Simone, A.; Camilloni, C.; Laio, A.; Vendruscolo, M., The inverted free energy landscape of an intrinsically disordered peptide by simulations and experiments. *Sci Rep* **2015,** *5*, 15449.
[26].Walti, M. A.; Orts, J.; Vogeli, B.; Campioni, S.; Riek, R., Solution NMR studies of recombinant Abeta(1-42): from the presence of a micellar entity to residual beta-sheet structure in the soluble species. *Chembiochem* **2015,** *16* (4), 659-69.
[27].Ebert, M. O.; Bae, S. H.; Dyson, H. J.; Wright, P. E., NMR relaxation study of the complex formed between CBP and the activation domain of the nuclear hormone receptor coactivator ACTR. *Biochemistry* **2008,** *47* (5), 1299-308.
[28].Iesmantavicius, V.; Jensen, M. R.; Ozenne, V.; Blackledge, M.; Poulsen, F. M.; Kjaergaard, M., Modulation of the intrinsic helix propensity of an intrinsically disordered protein reveals long-range helix-helix interactions. *Journal of the American Chemical Society* **2013,** *135* (27), 10155-63.
[29].Kjaergaard, M.; Norholm, A. B.; Hendus-Altenburger, R.; Pedersen, S. F.; Poulsen, F. M.; Kragelund, B. B., Temperature-dependent structural changes in intrinsically disordered proteins: formation of alpha-helices or loss of polyproline II? *Protein Sci* **2010,** *19* (8), 1555-64.
[30].Green, T. B.; Ganesh, O.; Perry, K.; Smith, L.; Phylip, L. H.; Logan, T. M.; Hagen, S. J.; Dunn, B. M.; Edison, A. S., IA3, an aspartic proteinase inhibitor from Saccharomyces cerevisiae, is intrinsically unstructured in solution. *Biochemistry* **2004,** *43* (14), 4071-81.
[31].Wong, T. S.; Rajagopalan, S.; Freund, S. M.; Rutherford, T. J.; Andreeva, A.; Townsley, F. M.; Petrovich, M.; Fersht, A. R., Biophysical characterizations of human mitochondrial transcription factor A and its binding to tumor suppressor p53. *Nucleic Acids Res* **2009,** *37* (20), 6765-83.
[32].Sibille, N.; Huvent, I.; Fauquant, C.; Verdegem, D.; Amniai, L.; Leroy, A.; Wieruszeski, J. M.; Lippens, G.; Landrieu, I., Structural characterization by nuclear magnetic resonance of the impact of phosphorylation in the proline-rich region of the disordered Tau protein. *Proteins* **2012,** *80* (2), 454-62.
[33].Honda, S.; Akiba, T.; Kato, Y. S.; Sawada, Y.; Sekijima, M.; Ishimura, M.; Ooishi, A.; Watanabe, H.; Odahara, T.; Harata, K., Crystal structure of a ten-amino acid protein. *Journal of the American Chemical Society* **2008,** *130* (46), 15327-31.
[34].Shalongo, W.; Dugad, L.; Stellwagen, E., Distribution of helicity within the model peptide acetyl (AAQAA) 3amide. *Journal of the American Chemical Society* **1994,** *116* (18), 8288-8293.
[35].Munoz, V.; Thompson, P. A.; Hofrichter, J.; Eaton, W. A., Folding dynamics and mechanism of β-hairpin formation. *Nature* **1997,** *390* (6656), 196.